Quantitative Finance

ISSN: 1469-7688 (Print) 1469-7696 (Online) Journal homepage: http://www.tandfonline.com/loi/rquf20

Rational multi-curve models with counterparty-risk valuation adjustments

Stéphane Crépey, Andrea Macrina, Tuyet Mai Nguyen & David Skovmand

To cite this article: Stéphane Crépey, Andrea Macrina, Tuyet Mai Nguyen & David Skovmand (2015): Rational multi-curve models with counterparty-risk valuation adjustments, Quantitative Finance, DOI: 10.1080/14697688.2015.1095348

To link to this article: http://dx.doi.org/10.1080/14697688.2015.1095348

Quantitative Finance, 2015
http://dx.doi.org/10.1080/14697688.2015.1095348

Routledge
Taylor & Francis Group

Rational multi-curve models with counterparty-risk valuation adjustments

STÉPHANE CRÉPEY†, ANDREA MACRINA*‡§, TUYET MAI NGUYEN† and DAVID SKOVMAND¶

†Laboratoire de Mathématiques et Modélisation d'Évry, Université Évry Val d'Essonne, Évry, France
‡Department of Mathematics, University College London, London, UK
§Department of Actuarial Science, University of Cape Town, Cape Town, South Africa
¶Department of Finance, Copenhagen Business School, Copenhagen, Denmark

(*Received 9 March 2015; accepted 3 September 2015; published online 17 November 2015*)

We develop a multi-curve term structure set-up in which the modelling ingredients are expressed by rational functionals of Markov processes. We calibrate to London Interbank Offer Rate swaptions data and show that a rational two-factor log-normal multi-curve model is sufficient to match market data with accuracy. We elucidate the relationship between the models developed and calibrated under a risk-neutral measure $\mathbb{Q}$ and their consistent equivalence class under the real-world probability measure $\mathbb{P}$. The consistent $\mathbb{P}$-pricing models are applied to compute the risk exposures which may be required to comply with regulatory obligations. In order to compute counterparty-risk valuation adjustments, such as credit valuation adjustment, we show how default intensity processes with rational form can be derived. We flesh out our study by applying the results to a basis swap contract.

Keywords: Multi-curve interest rate term structure models; LIBOR; Rational asset pricing models; Calibration; Counterparty-risk; Risk management; Markov functionals; Basis swap

1. Introduction

In this work, we endeavour to develop multi-curve interest rate models which extend to counterparty-risk models in a consistent fashion. The aim is the pricing and risk management of financial instruments with price models capable of discounting at multiple rates (e.g. overnight index swap (OIS) and London Interbank Offer Rate (LIBOR)) and which allow for corrections in the asset's valuation scheme so to adjust for counterparty-risk inclusive of credit, debt and liquidity risk. We thus propose factor models for (i) the OIS rate, (ii) the LIBOR and (iii) the default intensities of the two counterparties involved in bilateral OTC derivative transactions. The three ingredients are characterized by a feature they share in common: the rate and intensity models are all rational functions of the underlying factor processes. Since we have in mind the pricing of assets as well as the management of risk exposures, we also need to work within a set-up that maintains price consistency under various probability measures. We will, for instance, want to price derivatives by making use of a risk-neutral measure $\mathbb{Q}$ while analysing the statistics of risk exposures under the real-world measure $\mathbb{P}$. This point is particularly important when we calibrate the interest rate models to derivatives data, such as implied volatilities, and then apply the calibrated models to compute counterparty-risk valuation adjustments to comply with regulatory requirements. The presented rational models allow us to develop a comprehensive framework that begins with an OIS model, evolves to an approach for constructing the LIBOR process, includes the pricing of fixed-income assets and model calibration, analyses risk exposures and concludes with a credit risk model that is applied for the analysis of counterparty-risk valuation adjustments (XVA).

The issue of how to model multi-curve interest rates and incorporate counterparty-risk valuation adjustments in a pricing framework has motivated much research. For instance, research on multi-curve interest rate modelling is presented in Henrard (2007, 2010, 2014), Kijima *et al.* (2009), Kenyon (2010), Bianchetti (2010), Mercurio (2010b, 2010a, 2010c), Fujii *et al.* (2010, 2011), Bianchetti and Moreni (2013),

*Corresponding author. Email: a.macrina@ucl.ac.uk

Filipović and Trolle (2013), Moreni and Pallavicini (2014) or Crépey *et al.* (2015). On counterparty-risk valuation adjustment, we mention two recent books by Brigo *et al.* (2013) and Crépey *et al.* (2014); more references are given as we go along. Pricing models with rational form have appeared before. Flesaker and Hughston (1996) pioneered such pricing models and in particular introduced the so-called rational log-normal model for discount bond prices. Further related studies include Rutkowski (1997), Döberlein and Schweizer (2001) and Hunt and Kennedy (2004), Brody and Hughston (2005), Hughston and Rafailidis (2005), Brody *et al.* (2012), Parbhoo (2013), Akahori *et al.* (2014), Filipović *et al.* (2014), Macrina and Parbhoo (2014) or Nguyen and Seifried (2014). However, as far as we know, the present paper is the first to apply rational pricing models in a multi-curve set-up, along with Nguyen and Seifried (2014) who develop a rational multi-curve model in the spirit of Rogers (1997) based on a multiplicative spread, and it is the only rational pricing paper dealing with XVA computations. We shall see that, despite the simplicity of these models, they perform surprisingly well when comparing to other, in principle more elaborate, proposals such as Crépey *et al.* (2015) or Moreni and Pallavicini (2013, 2014). Other recent related research includes Filipović *et al.* (2014), for the study of unspanned volatility and its regulatory implications, Cuchiero *et al.* (2012), for moment computations in financial applications, and Cheng and Tehranchi (2014), motivated by stochastic volatility modelling.

This paper consists of three main parts: (a) development of the novel rational multi-curve interest rate approach along with the rational credit-intensity models necessary for the computation of the counterparty-risk valuation adjustments. This material is presented in section 2. (b) Clean valuation of interest rate securities and model calibration (sections 3 and 4), where we consider specific rational factor models for the multi-curve interest rates and default intensity models with the goal in mind of singling out the 'most' parsimonious model that best calibrates to available derivatives data. (c) Counterparty-risk valuation adjustments (section 5), which are computed for basis swaps priced with the rational rate models. The basis swap case study gives also the opportunity to highlight the importance of consistent pricing and hedging under $\mathbb{P}$ and $\mathbb{Q}$.

The main novel research contributions are listed as follows: (i) the *rational models for multi-curve term structures* whereby we derive the *LIBOR process* by pricing a forward rate agreement (FRA) under the real-world probability measure. In doing so, we apply a pricing kernel model. The short rate model arising from the pricing kernel process is taken as a proxy model for the OIS rate. In view of derivative pricing in subsequent sections, we also provide an alternative derivation of the rational multi-curve interest rate models by starting with the risk-neutral measure. We call this method *bottom-up risk-neutral approach*. (ii) We explain the advantages one gains from the resulting *'codebook' for the LIBOR process*, which we model as a rational function where the denominator is the stochastic discount factor associated with the utilized probability measure. We calibrate three specifications of our multi-curve framework and assess them for the quality of fit and on positivity of rates and spread. We show that a one-factor rational model is too rigid to be able to calibrate the given data, a shortcoming that one cannot get rid of even when the driving factor features jumps in its dynamics. We conclude by emphasising a *two-factor log-normal OIS-LIBOR model* as the 'most' parsimonious rational model with good tractability and calibration properties. To our knowledge, this is the first time such an in-depth calibration analysis has been performed on rational interest rate models. (iii) We show the explicit relationship in our set-up between pricing under an equivalent measure and the real-world probability measure. We compute the risk exposure associated with holding a basis swap and plot the quantiles under both probability measures for comparison. As an example, we apply Lévy random bridges to describe the dynamics of the factor processes under $\mathbb{P}$. This enables us to interpret the re-weighting of the risk exposure under $\mathbb{P}$ as an effect that could be related to, e.g., 'forward guidance' provided by a central bank. (iv) We propose new *credit default intensity models with rational form*, which can be guaranteed to take positive values at all times and have the same appealing mathematical tractability as the rational (multi-curve) interest rate models. (v) We compute *XVA*, that is, the counterparty-risk valuation adjustments due to credit, debt and liquidity risk, *based on rational multi-curve interest rate and rational credit-intensity models*.

2. Rational multi-curve term structures

We model a financial market by a filtered probability space $(\Omega, \mathcal{F}, \mathbb{P}, \{\mathcal{F}_t\}_{0\le t})$, where $\mathbb{P}$ denotes the real probability measure and $\{\mathcal{F}_t\}_{0\le t}$ is the market filtration. The no-arbitrage pricing formula for a generic (non-dividend-paying) financial asset with price process $\{S_{tT}\}_{0\le t\le T}$, which is characterized by a cash flow S_{TT} at the fixed date T, is given by

$$S_{tT} = \frac{1}{\pi_t}\mathbb{E}^{\mathbb{P}}[\pi_T S_{TT} \mid \mathcal{F}_t], \tag{2.1}$$

where $\{\pi_t\}_{0\le t\le U}$ is the pricing kernel embodying the inter-temporal discounting and risk-adjustments, see e.g. Hunt and Kennedy (2004). Once the model for the pricing kernel is specified, the OIS discount bond price process $\{P_{tT}\}_{0\le t\le T}$ is determined as a special case of formula (2.1) by

$$P_{tT} = \frac{1}{\pi_t}\mathbb{E}^{\mathbb{P}}[\pi_T \mid \mathcal{F}_t]. \tag{2.2}$$

The associated OIS short rate of interest is obtained by

$$r_t = -\left(\partial_T \ln P_{tT}\right)|_{T=t}, \tag{2.3}$$

where it is assumed that the discount bond system is differentiable in its maturity parameter T. The rate $\{r_t\}$ is non-negative if the pricing kernel $\{\pi_t\}$ is a supermartingale and vice versa. We next go on to infer a pricing formula for financial

derivatives written on LIBOR. In doing so, we also derive a price process (2.6) that we identify as determining the dynamics of the FRA rate (2.7). It is this formula that, in our work, reveals the nature of the so-called multi-curve term structure, whereby the OIS rate and the LIBOR rates of different tenors are treated as distinct discount rates.

2.1. Generic multi-curve interest rate models

We propose a new method for constructing multi-curve pricing models for securities written on LIBOR by starting with the valuation of a FRA. We consider $0 \le t \le T_0 \le T_2 \le \cdots \le T_i \le \cdots \le T_n$, where $T_0, T_i, \ldots, T_n$ are fixed dates, and let N be a notional, K a strike rate and $\delta_i = T_i - T_{i-1}$. The fixed leg of the FRA contract is given by $NK\delta_i$ and the floating leg payable in arrears at time T_i is modelled by $N\delta_i L(T_i; T_{i-1}, T_i)$, where the random rate $L(T_i; T_{i-1}, T_i)$ is $\mathcal{F}_{T_{i-1}}$ measurable. The net cash flow at the maturity date T_i of the FRA contract reads

$$H_{T_i} = N\delta_i \left[K - L(T_i; T_{i-1}, T_i)\right]. \tag{2.4}$$

The FRA price process is then given by an application of (2.1), that is, for $0 \le t \le T_{i-1}$, by

$$\begin{aligned} H_{tT_i} &= \frac{1}{\pi_t}\mathbb{E}^{\mathbb{P}}\left[\pi_{T_i} H_{T_i} \,\middle|\, \mathcal{F}_t\right] \\ &= N\delta_i \left[K P_{tT_i} - L(t, T_{i-1}, T_i)\right], \end{aligned} \tag{2.5}$$

where we define

$$L(t; T_{i-1}, T_i) := \frac{1}{\pi_t}\mathbb{E}^{\mathbb{P}}\left[\pi_{T_i} L(T_i; T_{i-1}, T_i) \,\middle|\, \mathcal{F}_t\right]. \tag{2.6}$$

We call the above process the *LIBOR process*. We note here that even though LIBOR is not as such a traded asset, the process (2.6) may be interpreted as a 'price process' of a tradable asset with cash flow $L(T_i; T_{i-1}, T_i)$ at time T_i. The fair spread of the FRA at time t (the value of K at time t such that $H_{tT_i} = 0$), called the *FRA rate* is then expressed in terms of $L(t; T_{i-1}, T_i)$ by

$$K_t = \frac{L(t; T_{i-1}, T_i)}{P_{tT_i}}. \tag{2.7}$$

For times up to and including T_{i-1}, the LIBOR process (2.6) can be written in terms of a conditional expectation of an $\mathcal{F}_{T_{i-1}}$-measurable random variable. In fact, for $t \le T_{i-1}$,

$$\begin{aligned} &\mathbb{E}^{\mathbb{P}}\left[\pi_{T_i} L(T_i; T_{i-1}, T_i) \,\middle|\, \mathcal{F}_t\right] \\ &\quad = \mathbb{E}^{\mathbb{P}}\left[\mathbb{E}^{\mathbb{P}}\left[\pi_{T_i} L(T_i; T_{i-1}, T_i) \,\middle|\, \mathcal{F}_{T_{i-1}}\right] \,\middle|\, \mathcal{F}_t\right] \end{aligned} \tag{2.8}$$

$$= \mathbb{E}^{\mathbb{P}}\left[\mathbb{E}^{\mathbb{P}}\left[\pi_{T_i} \,\middle|\, \mathcal{F}_{T_{i-1}}\right] L(T_i; T_{i-1}, T_i) \,\middle|\, \mathcal{F}_t\right], \tag{2.9}$$

and thus

$$L(t, T_{i-1}, T_i) = \frac{1}{\pi_t}\mathbb{E}^{\mathbb{P}}\left[\mathbb{E}^{\mathbb{P}}\left[\pi_{T_i} \,\middle|\, \mathcal{F}_{T_{i-1}}\right] L(T_i; T_{i-1}, T_i) \,\middle|\, \mathcal{F}_t\right]. \tag{2.10}$$

The (pre-crisis) classical approach to LIBOR modelling defines the price process $\{H_{tT_i}\}$ of a FRA by

$$H_{tT_i} = N\left[(1 + \delta_i K) P_{tT_i} - P_{tT_{i-1}}\right], \tag{2.11}$$

see, e.g. Hunt and Kennedy (2004). By equating with (2.5), we see that the classical single-curve LIBOR model is obtained in the special case where

$$L(t; T_{i-1}, T_i) = \frac{1}{\delta_i}\left(P_{tT_{i-1}} - P_{tT_i}\right). \tag{2.12}$$

Remark 2.1 Unless markets feature inverted yield curves, one expects the positive spread relation $L(t; T, T + \delta_i) < L(t; T, T + \delta_j)$, for tenors $\delta_j > \delta_i$, to hold . We shall return to this relationship in section 4, where various model specifications are calibrated and the positivity of the spread is checked. For recent work on multi-curve modelling with focus on spread modelling, we refer to Cuchiero *et al.* (2014).

2.2. Multi-curve models with rational form

In order to construct explicit LIBOR processes, the pricing kernel $\{\pi_t\}$ and the random variable $L(T_i; T_{i-1}, T_i)$ need to be specified in the definition (2.6). For reasons that will become apparent as we move forward in this paper—including mathematical tractability, good calibration properties and parsimonious modelling—we opt to apply the rational pricing models for a generic financial asset proposed in Macrina (2014). These models bestow a rational form on the price processes, here intended as a 'quotient of summands' (slightly abusing the terminology that usually refers to a 'quotient of polynomials'). The basic pricing model with rational form for a generic financial asset (for short 'rational pricing model') that we borrow here is given by

$$S_{tT} = \frac{S_{0T} + b_2(T)A_t^{(2)} + b_3(T)A_t^{(3)}}{P_{0t} + b_1(t)A_t^{(1)}}, \tag{2.13}$$

where S_{0T} is the value of the asset at $t = 0$. There may be more bA-terms in the numerator, but two (at most) will be enough for all our purposes in this work. For $0 \le t \le T$ and $i = 1, 2, 3$, $b_i(t)$ are deterministic functions and $A_t^{(i)} = A_i(t, X_t^{(i)})$ are martingale processes, not necessarily under $\mathbb{P}$, but under an equivalent martingale measure $\mathbb{M}$, which are driven by $\mathbb{M}$-Markov processes $\{X_t^{(i)}\}$. The details of how the expression (2.13) is derived from the formula (2.1), and in particular how explicit examples for $\{A_t^{(i)}\}$ can be constructed, are shown in Macrina (2014). Having opted for the particular rational pricing model (2.13), it follows from the relation (2.1) that the pricing kernel model associated with the price process (2.13) necessarily has the form

$$\pi_t = \frac{\pi_0}{M_0}\left[P_{0t} + b_1(t)A_t^{(1)}\right] M_t, \tag{2.14}$$

where $\{M_t\}$ is the $\mathbb{P}$-martingale that induces the change of measure from $\mathbb{P}$ to an auxiliary measure $\mathbb{M}$, under which the $\{A_t^{(i)}\}$ are martingales. The deterministic functions P_{0t} and $b_1(t)$ are defined such that $P_{0t} + b_1(t)A_t^{(1)}$ is a non-negative $\mathbb{M}$-supermartingale (see e.g. example 2.1), and thus in such a way that $\{\pi_t\}$ is a non-negative $\mathbb{P}$-supermartingale. By the equations (2.2) and (2.3), it is straightforward to see that

$$P_{tT} = \frac{P_{0T} + b_1(T)A_t^{(1)}}{P_{0t} + b_1(t)A_t^{(1)}}, \quad r_t = -\frac{\dot{P}_{0t} + \dot{b}_1(t)A_t^{(1)}}{P_{0t} + b_1(t)A_t^{(1)}}, \tag{2.15}$$

where the 'dot-notation' means differentiation with respect to time t.

Let us return to the modelling of rational multi-curve term structures and in particular to the definition of the (forward) LIBOR process. Putting equations (2.6) and (2.1) in relation, we see that the class of models (2.13) naturally lends itself for the modelling of the LIBOR process (2.6) in the considered set-up. Since (2.13) satisfies (2.1) by construction, so does the LIBOR model

$$L(t; T_{i-1}, T_i) = \frac{L(0; T_{i-1}, T_i) + b_2(T_{i-1}, T_i)A_t^{(2)} + b_3(T_{i-1}, T_i)A_t^{(3)}}{P_{0t} + b_1(t)A_t^{(1)}} \tag{2.16}$$

satisfy the martingale equation (2.6) and in particular (2.10) for $t \le T_{i-1}$. Based on our knowledge, this is the first time that LIBOR is modelled in this way. In Macrina (2014), a method based on the use of weighted heat kernels is provided for the explicit construction of the $\mathbb{M}$-martingales $\{A_t^{(i)}\}_{i=1,2}$. This further application allows for the development of (explicit) LIBOR processes, which, if circumstances in financial markets require it, by construction takes positive values at all times.

2.3. *Bottom-up risk-neutral approach*

Since we also deal with counterparty-risk valuation adjustments, we present another scheme for the construction of the LIBOR models, which we call 'bottom-up risk-neutral approach'. As the name suggests, we model the multi-curve term structure by making use of the risk-neutral measure (via the auxiliary measure $\mathbb{M}$), while the connection to the $\mathbb{P}$-dynamics of prices can be reintroduced at a later stage, which is important for the calculation of risk exposures and their management. 'Bottom-up' refers to the fact that the short interest rate will be modelled first, then followed by the discount bond price and LIBOR processes. Similarly, in section 2.4, the default intensity processes will be modelled first, and thereafter the price processes of counterparty-risky assets will be derived thereof. We utilize the notation $\mathbb{E}[\ldots|\mathcal{F}_t] = \mathbb{E}_t[\ldots]$. In the bottom-up setting, we directly model the short risk-free rate $\{r_t\}$ in the manner of the right-hand side in (2.15), i.e.

$$r_t = -\frac{\dot{c}_1(t) + \dot{b}_1(t)A_t^{(1)}}{c_1(t) + b_1(t)A_t^{(1)}}, \tag{2.17}$$

by postulating (i) non-increasing deterministic functions $b_1(t)$ and $c_1(t)$ with $c_1(0) = 1$ (later $c_1(t)$ will be seen to coincide with P_{0t}) and (ii) an $(\{\mathcal{F}_t\}, \mathbb{M})$-martingale $\{A_t^{(1)}\}$ with $A_0^{(1)} = 0$ such that

$$h_t = c_1(t) + b_1(t)A_t^{(1)} \tag{2.18}$$

is a positive $(\{\mathcal{F}_t\}, \mathbb{M})$-supermartingale for all $t > 0$.

Example 2.1 Let $A_t^{(1)} = S_t^{(1)} - 1$, where $\{S_t^{(1)}\}$ is a positive $\mathbb{M}$-martingale with $S_0^{(1)} = 1$, for example, a unit-initialized exponential Lévy martingale. Then, the supermartingale (2.18) is positive for any given t if $0 < b_1(t) \le c_1(t)$.

Associated with the supermartingale (2.18), we characterize the (risk-neutral) pricing measure $\mathbb{Q}$ by the $\mathbb{M}$-density process $\{\mu_t\}_{0\le t\le T}$, given by

$$\mu_t = \frac{\mathrm{d}\mathbb{Q}}{\mathrm{d}\mathbb{M}}\Big|_{\mathcal{F}_t} = \mathcal{E}\left(\int_0^t \frac{b_1(s)\mathrm{d}A_s^{(1)}}{c_1(s) + b_1(s)A_{s-}^{(1)}}\right), \tag{2.19}$$

which is taken to be a positive $(\{\mathcal{F}_t\}, \mathbb{M})$-martingale. We note that, in principle, we allow for jumps in this set-up, and thus we denote by $\{A_{t-}^{(1)}\}$ the left-limit process of $\{A_t^{(1)}\}$, where all semi-martingales are assumed right continuous with left limits. Furthermore, we denote by $D_t = \exp\left(-\int_0^t r_s\,\mathrm{d}s\right)$ the discount factor associated with the risk-neutral measure $\mathbb{Q}$.

LEMMA 2.1 $h_t = D_t\,\mu_t$.

Proof The Ito semi-martingale formula applied to $\varphi(t, A_t^{(1)}) = \ln(c_1(t) + b_1(t)A_t^{(1)}) = \ln(h_t)$ and to $\ln(D_t\mu_t)$ gives the following relations:

$$\begin{aligned}
&\mathrm{d}\ln\left(c_1(t) + b_1(t)A_t^{(1)}\right) \\
&= -r_t\mathrm{d}t + \frac{b_1(t)\mathrm{d}A_t^{(1)}}{c_1(t) + b_1(t)A_{t-}^{(1)}} - \frac{b_1^2(t)\mathrm{d}[A^{(1)}, A^{(1)}]_t^c}{2(c_1(t) + b_1(t)A_{t-}^{(1)})^2} \\
&\quad + \mathrm{d}\sum_{s\le t}\left(\Delta\ln\left(c_1(t) + b_1(t)A_t^{(1)}\right) - \frac{b_1(t)\Delta A_t^{(1)}}{c_1(t) + b_1(t)A_{t-}^{(1)}}\right),
\end{aligned} \tag{2.20}$$

where (2.17) was used in the first line, and

$$\begin{aligned}
\mathrm{d}\ln(D_t\mu_t) &= \mathrm{d}\ln D_t + d\ln\mu_t \\
&= -r_t\mathrm{d}t + \frac{\mathrm{d}\mu_t}{\mu_{t-}} - \frac{\mathrm{d}[\mu,\mu]_t^c}{2(\mu_{t-})^2} \\
&\quad + \mathrm{d}\sum_{s\le t}\left(\Delta\ln(\mu_t) - \frac{\Delta\mu_t}{\mu_{t-}}\right) \\
&= -r_t\mathrm{d}t + \frac{b_1(t)\mathrm{d}A_t^{(1)}}{c_1(t) + b_1(t)A_{t-}^{(1)}} \\
&\quad - \frac{b_1^2(t)\mathrm{d}[A^{(1)}, A^{(1)}]_t^c}{2(c_1(t) + b_1(t)A_{t-}^{(1)})^2} \\
&\quad + \mathrm{d}\sum_{s\le t}\left(\Delta\ln(\mu_t) - \frac{b_1(t)\Delta A_t^{(1)}}{c_1(t) + b_1(t)A_{t-}^{(1)}}\right),
\end{aligned} \tag{2.21}$$

where

$$\begin{aligned}
\Delta\ln(\mu_t) &= \ln\left(\frac{\mu_t}{\mu_{t-}}\right) = \ln\left(1 + \frac{b_1(t)\Delta A_t^{(1)}}{c_1(t) + b_1(t)A_{t-}^{(1)}}\right) \\
&= \ln\left(\frac{c_1(t) + b_1(t)A_t^{(1)}}{c_1(t) + b_1(t)A_{t-}^{(1)}}\right) \\
&= \Delta\ln\left(c_1(t) + b_1(t)A_t^{(1)}\right).
\end{aligned}$$

Therefore, $\mathrm{d}\ln(h_t) = \mathrm{d}\ln(D_t\mu_t)$. Moreover, $h_0 = D_0\mu_0 = 1$. Hence, $h_t = D_t\mu_t$. □

It then follows that the price process of the OIS discount bond with maturity T can be expressed, for $0 \le t \le T$, by

$$P_{tT} = \mathbb{E}_t^{\mathbb{Q}}\left[\frac{D_T}{D_t}\right] = \frac{1}{D_t\,\mu_t}\mathbb{E}^{\mathbb{M}}\left[D_T\,\mu_T \mid \mathcal{F}_t\right] = \mathbb{E}_t^{\mathbb{M}}\left[\frac{h_T}{h_t}\right] = \frac{c_1(T) + b_1(T)A_t^{(1)}}{c_1(t) + b_1(t)A_t^{(1)}}. \tag{2.22}$$

Thus, the process $\{h_t\}$ plays the role of the pricing kernel associated with the OIS market under the measure $\mathbb{M}$. In particular, we note that $c_1(t) = P_{0t}$ for $t \in [0, T]$ and $r_t = -(\partial_T \ln P_{tT})_{|T=t}$. A construction inspired by the above formula for the OIS bond leads to the rational model for the LIBOR prevailing over the interval $[T_{i-1}, T_i)$. The $\mathcal{F}_{T_{i-1}}$-measurable spot LIBOR rate $L(T_i; T_{i-1}, T_i)$ is modelled in terms of $\{A_t^{(1)}\}$ and, in this paper, at most two other $\mathbb{M}$-martingales $\{A_t^{(2)}\}$ and $\{A_t^{(3)}\}$ evaluated at T_{i-1}:

$$L(T_i; T_{i-1}, T_i) = \frac{L(0; T_{i-1}, T_i) + b_2(T_{i-1}, T_i)A_{T_{i-1}}^{(2)} + b_3(T_{i-1}, T_i)A_{T_{i-1}}^{(3)}}{P_{0T_i} + b_1(T_i)A_{T_{i-1}}^{(1)}}. \tag{2.23}$$

The (forward) LIBOR process is then defined by an application of the risk-neutral valuation formula (which is equivalent to the pricing formula (2.1) under $\mathbb{P}$) as follows. For $t \le T_{i-1}$, we let

$$L(t; T_{i-1}, T_i) = \frac{1}{D_t}\mathbb{E}_t^{\mathbb{Q}}\left[D_{T_i}\,L(T_i; T_{i-1}, T_i)\right] = \mathbb{E}_t^{\mathbb{M}}\left[\frac{D_{T_i}\,\mu_{T_i}}{D_t\,\mu_t}\,L(T_i; T_{i-1}, T_i)\right] \tag{2.24}$$

$$= \mathbb{E}_t^{\mathbb{M}}\left[\frac{\mathbb{E}_{T_{i-1}}^{\mathbb{M}}[h_{T_i}]L(T_i; T_{i-1}, T_i)}{h_t}\right], \tag{2.25}$$

and thus, by applying (2.18) and (2.23),

$$L(t; T_{i-1}, T_i) = \frac{L(0; T_{i-1}, T_i) + b_2(T_{i-1}, T_i)A_t^{(2)} + b_3(T_{i-1}, T_i)A_t^{(3)}}{P_{0t} + b_1(t)A_t^{(1)}}. \tag{2.26}$$

Hence, we recover the same model and expression as in (2.16). The LIBOR models (2.26) (or (2.16)) are compatible with an HJM multi-curve set-up where, in the spirit of Heath *et al.* (1992), the initial term structures P_{0T_i} and $L(0; T_{i-1}, T_i)$ are fitted by construction.

Example 2.2 Let $A_t^{(i)} = S_t^{(i)} - 1$, where $S_t^{(i)}$ is a positive $\mathbb{M}$-martingale with $S_0^{(i)} = 1$. For example, one could consider a unit-initialized exponential Lévy martingale defined in terms of a function of an $\mathbb{M}$-Lévy process $\{X_t^{(i)}\}$, for $i = 2, 3$. Such a construction produces non-negative LIBOR rates if

$$0 \le b_2(T_{i-1}, T_i) + b_3(T_{i-1}, T_i) \le L(0; T_{i-1}, T_i). \tag{2.27}$$

If this condition is not satisfied, then the LIBOR model may be viewed as a shifted model, in which the LIBOR rates may become negative with positive probability. For different kinds of shifts used in the multi-curve term structure literature, we refer to, e.g. Mercurio (2010a) or Moreni and Pallavicini (2014).

2.4. Rational credit model

For the counterparty-risk valuation adjustments (XVA) produced later in this paper, we require credit-intensity models, which we construct in the same fashion as the rational multi-curve interest rate models. The following novel rational default-intensity models are developed by use of the 'bottom-up risk-neutral approach' presented in the previous section.

We consider $\{X_t^{(i)}\}_{t\ge 0}^{i=1,2,\ldots,n}$, which are assumed to be $(\{\mathcal{F}_t\}, \mathbb{M})$-Markov processes. For any multi-index $(i_1, \ldots, i_d)$, we write $\mathcal{F}_t^{(i_1,\ldots,i_d)} = \bigvee_{l=1,\ldots,d} \mathcal{F}_t^{X^{(i_l)}}$. The (market) filtration $\{\mathcal{F}_t\}$ is given by $\{\mathcal{F}_t^{(1,\ldots,n)}\}$. For the application in the present section, we fix $n = 6$. Markov processes $\{X_t^{(1)}\} = \{X^{(3)}\}$ and $\{X_t^{(2)}\}$ are utilized to drive the OIS and LIBOR models as described in section 2.3, in particular the zero-initialized $(\{\mathcal{F}_t\}, \mathbb{M})$-martingales $\{A_t^{(i)}\}^{i=1,2,3}$. The Markov processes $\{X_t^{(i)}\}$, $i = 4, 5, 6$, which are assumed to be mutually $\mathbb{M}$-independent as well as $\mathbb{M}$-independent of the Markov processes $i = 1, 2, 3$, are applied to model $\{\mathcal{F}_t\}$-adapted processes $\{\gamma_t^{(i)}\}^{i=4,5,6}$ defined by

$$\gamma_t^{(i)} = -\frac{\dot{c}_i(t) + \dot{b}_i(t)A_t^{(i)}}{c_i(t) + b_i(t)A_t^{(i)}}, \tag{2.28}$$

where $b_i(t)$ and $c_i(t)$, with $c_i(0) = 1$, are non-increasing deterministic functions, and where $\{A_t^{(i)}\}^{i=4,5,6}$ are zero-initialized $(\{\mathcal{F}_t\}, \mathbb{M})$-martingales of the form $A(t, X_t^{(i)})$. Comparing with (2.17), we see that (2.28) is modelled in the same way as the OIS rate (2.17), non-negative in particular, as an intensity should be (see remark 2.2).

In line with the 'bottom-up' construction in section 2.3, we now introduce a density $(\{\mathcal{F}_t\}, \mathbb{M})$-martingale $\{\mu_t \nu_t\}_{0\le t\le T}$ that induces a measure change from $\mathbb{M}$ to the risk-neutral measure $\mathbb{Q}$:

$$\left.\frac{\mathrm{d}\mathbb{Q}}{\mathrm{d}\mathbb{M}}\right|_{\mathcal{F}_t} = \mu_t \nu_t \quad 0 \le t \le T,$$

where $\{\mu_t\}$ is defined as in section 2.3. Here, we furthermore define $\nu_t = \prod_{i\ge 4} \nu_t^{(i)}$, where the processes

$$\nu_t^{(i)} = \mathcal{E}\left(\int_0^{\cdot} \frac{\dot{b}_i(t)\mathrm{d}A_t^{(i)}}{\dot{c}_i(t) + \dot{b}_i(t)A_{t-}^{(i)}}\right)$$

are assumed to be positive true $(\{\mathcal{F}_t\}, \mathbb{M})$-martingales.

LEMMA 2.2 *Let ξ denote any non-negative $\mathcal{F}_T^{(1,2,3)}$-measurable random variable and let $\chi = \prod_{j\ge 4} \chi_i$ where, for $j = 4, 5, 6$, χ_j is $\mathcal{F}_T^{(j)}$-measurable. Then,*

$$\mathbb{E}_t^{\mathbb{R}}[\xi\,\chi] = \mathbb{E}_t^{\mathbb{R}}[\xi]\prod_{j\ge 4}\mathbb{E}_t^{\mathbb{R}}[\chi_i], \tag{2.29}$$

for $\mathbb{R} = \mathbb{M}$ or $\mathbb{Q}$ and for $0 \le t \le T$.

Proof Since $\mathcal{F}_T^{(4,5,6)}$ is independent of $\mathcal{F}_t^{(1,2,3)}$ and of ξ,

$$\mathbb{E}^{\mathbb{M}}\left[\xi \mid \mathcal{F}_t^{(1,2,3)} \vee \mathcal{F}_T^{(4,5,6)}\right] = \mathbb{E}^{\mathbb{M}}\left[\xi \mid \mathcal{F}_t^{(1,2,3)}\right].$$

Therefore,

$$\begin{aligned}
&\mathbb{E}_t^{\mathbb{M}}[\xi\,\chi]\\
&= \mathbb{E}^{\mathbb{M}}\left[\mathbb{E}^{\mathbb{M}}\left[\xi\,\chi \,\middle|\, \mathcal{F}_t^{(1,2,3)} \vee \mathcal{F}_T^{(4,5,6)}\right] \,\middle|\, \mathcal{F}_t^{(1,2,3)} \vee \mathcal{F}_t^{(4,5,6)}\right]\\
&= \mathbb{E}^{\mathbb{M}}\left[\mathbb{E}^{\mathbb{M}}\left[\xi \,\middle|\, \mathcal{F}_t^{(1,2,3)} \vee \mathcal{F}_T^{(4,5,6)}\right]\chi \,\middle|\, \mathcal{F}_t^{(1,2,3)} \vee \mathcal{F}_t^{(4,5,6)}\right]\\
&= \mathbb{E}^{\mathbb{M}}\left[\mathbb{E}^{\mathbb{M}}\left[\xi \,\middle|\, \mathcal{F}_t^{(1,2,3)}\right]\chi \,\middle|\, \mathcal{F}_t^{(1,2,3)} \vee \mathcal{F}_t^{(4,5,6)}\right]\\
&= \mathbb{E}^{\mathbb{M}}\left[\xi \,\middle|\, \mathcal{F}_t^{(1,2,3)}\right]\mathbb{E}^{\mathbb{M}}\left[\chi \,\middle|\, \mathcal{F}_t^{(1,2,3)} \vee \mathcal{F}_t^{(4,5,6)}\right]\\
&= \mathbb{E}_t^{\mathbb{M}}[\xi]\,\mathbb{E}_t^{\mathbb{M}}[\chi]\,.
\end{aligned}$$

Next, the Girsanov formula in combination with the result for $\mathbb{M}$-conditional expectation yields:

$$\begin{aligned}
\mathbb{E}_t^{\mathbb{Q}}[\xi\chi] &= \mathbb{E}_t^{\mathbb{M}}\left[\frac{\mu_T \nu_T \xi\chi}{\mu_t \nu_t}\right] = \mathbb{E}_t^{\mathbb{M}}\left[\frac{\mu_T \xi}{\mu_t}\right]\mathbb{E}_t^{\mathbb{M}}\left[\frac{\nu_T \chi}{\nu_t}\right]\\
&= \mathbb{E}_t^{\mathbb{M}}\left[\frac{\nu_T \mu_T \xi}{\nu_t \mu_t}\right]\mathbb{E}_t^{\mathbb{M}}\left[\frac{\mu_T \nu_T \chi}{\mu_t \nu_t}\right] = \mathbb{E}_t^{\mathbb{Q}}[\xi]\,\mathbb{E}_t^{\mathbb{Q}}[\chi]\,.
\end{aligned}$$

The result remains to be proven for the case $\xi = 1$, which is done similarly. □

For the XVA computations, we shall use a reduced-form counterparty-risk approach, where the default times of a bank 'b' (we adopt its point of view) and of its counterparty 'c' are modeled in terms of three Cox times τ_i defined by

$$\tau_i = \inf\left\{t > 0 \,\middle|\, \int_0^t \gamma_s^{(i)}\,\mathrm{d}s \geq E_i\right\}. \tag{2.30}$$

Under $\mathbb{Q}$, the random variables E_i $(i = 4, 5, 6)$ are independent and exponentially distributed. Furthermore, $\tau_c = \tau_4 \wedge \tau_6$ $\tau_b = \tau_5 \wedge \tau_6$, hence $\tau = \tau_b \wedge \tau_c = \tau_4 \wedge \tau_5 \wedge \tau_6$.

We write

$$\gamma_t^c = \gamma_t^{(4)} + \gamma_t^{(6)}\ \gamma_t^b = \gamma_t^{(5)} + \gamma_t^{(6)}\ \gamma_t = \gamma_t^{(4)} + \gamma_t^{(5)} + \gamma_t^{(6)},$$

which are the so-called $(\{\mathcal{F}_t\}, \mathbb{Q})$-hazard intensity processes of the $\{\mathcal{G}_t\}$ stopping times τ_c, τ_b and τ, where the full model filtration $\{\mathcal{G}_t\}$ is given as the market filtration $\{\mathcal{F}_t\}$-progressively enlarged by τ_c and τ_b (see, e.g. Bielecki *et al.* (2009), Chapter 5). Writing as before $D_t = \exp(-\int_0^t r_s\,\mathrm{d}s)$, we note that lemma 2.1 still holds in the present set-up. That is,

$$h_t = c_1(t) + b_1(t)A_t^{(1)} = D_t\,\mu_t,$$

an $(\{\mathcal{F}_t\}, \mathbb{M})$-supermartingale, assumed to be positive (e.g. under an exponential Lévy martingale specification for $\{A_t^{(1)}\}$ as in example 2.2). Further, we introduce $Z_t^{(i)} = \exp(-\int_0^t \gamma_s^{(i)}\,\mathrm{d}s)$, for $i = 4, 5, 6$, and obtain analogously that

$$k_t^{(i)} := c_i(t) + b_i(t)A_t^{(i)} = Z_t^i\,\nu_t^{(i)}. \tag{2.31}$$

With these observations at hand, the following results follow from Lemma 2.2. We write $k_t = \prod_{i\geq 4} k_t^{(i)}$ and $Z_t = \prod_{i\geq 4} Z_t^{(i)}$.

Proposition 2.1 *The identities* (2.22) *and* (2.26) *still hold in the present set-up, that is*

$$\begin{aligned}
P_{tT} = \mathbb{E}_t^{\mathbb{Q}}\left[\mathrm{e}^{-\int_t^T r_s\,\mathrm{d}s}\right] &= \mathbb{E}_t^{\mathbb{Q}}\left[\frac{D_T}{D_t}\right] = \mathbb{E}_t^{\mathbb{M}}\left[\frac{h_T}{h_t}\right]\\
&= \frac{c_1(T) + b_1(T)A_t^{(1)}}{c_1(t) + b_1(t)A_t^{(1)}}
\end{aligned} \tag{2.32}$$

and, for $t \leq T_{i-1}$,

$$\begin{aligned}
&L(t; T_{i-1}, T_i)\\
&= \frac{L(0; T_{i-1}, T_i) + b_2(T_{i-1}, T_i)A_t^{(2)} + b_3(T_{i-1}, T_i)A_t^{(3)}}{P_{0t} + b_1(t)A_t^{(1)}}.
\end{aligned} \tag{2.33}$$

Likewise,

$$\begin{aligned}
\mathbb{E}_t^{\mathbb{Q}}\left[\mathrm{e}^{-\int_t^T \gamma_s\,\mathrm{d}s}\right] &= \mathbb{E}_t^{\mathbb{Q}}\left[\frac{Z_T}{Z_t}\right] = \mathbb{E}_t^{\mathbb{M}}\left[\frac{k_T}{k_t}\right]\\
&= \prod_{i=4,5,6} \frac{c_i(T) + b_i(T)A_t^{(i)}}{c_i(t) + b_i(t)A_t^{(i)}},
\end{aligned} \tag{2.34}$$

$$\begin{aligned}
\mathbb{E}_t^{\mathbb{Q}}\left[\mathrm{e}^{-\int_t^T \gamma_s\,\mathrm{d}s}\,\gamma_T^c\right] &= -\mathbb{E}_t^{\mathbb{Q}}\left[\frac{Z_T^{(5)}}{Z_t^{(5)}}\right]\partial_T\,\mathbb{E}_t^{\mathbb{Q}}\left[\frac{Z_T^{(4)}Z_T^{(6)}}{Z_t^{(4)}Z_t^{(6)}}\right]\\
&= -\mathbb{E}_t^{\mathbb{Q}}\left[\mathrm{e}^{-\int_t^T \gamma_s\,\mathrm{d}s}\right]\sum_{i=4,6}\frac{\dot{c}_i(T) + \dot{b}_i(T)A_t^{(i)}}{c_i(t) + b_i(t)A_t^{(i)}},
\end{aligned} \tag{2.35}$$

$$\begin{aligned}
\mathbb{E}_t^{\mathbb{Q}}\left[\mathrm{e}^{-\int_t^T (r_s+\gamma_s^c)\mathrm{d}s}\right] &= \mathbb{E}_t^{\mathbb{Q}}\left[\frac{D_T Z_T^{(4)} Z_T^{(6)}}{D_t Z_t^{(4)} Z_t^{(6)}}\right]\\
&= \prod_{i=1,4,6}\frac{c_i(T) + b_i(T)A_t^{(i)}}{c_i(t) + b_i(t)A_t^{(i)}}.
\end{aligned} \tag{2.36}$$

Proof Using lemma 2.2, we compute

$$\begin{aligned}
\mathbb{E}_t^{\mathbb{Q}}\left[\mathrm{e}^{-\int_t^T r_s\mathrm{d}s}\right] &= \mathbb{E}_t^{\mathbb{Q}}\left[\frac{D_T}{D_t}\right] = \mathbb{E}_t^{\mathbb{M}}\left[\frac{h_T \nu_T}{h_t \nu_t}\right]\\
&= \mathbb{E}_t^{\mathbb{M}}\left[\frac{h_T}{h_t}\right]\mathbb{E}_t^{\mathbb{M}}\left[\frac{\nu_T}{\nu_t}\right]\\
&= \mathbb{E}_t^{\mathbb{M}}\left[\frac{h_T}{h_t}\right] = \frac{c_1(T) + b_1(T)A_t^{(1)}}{c_1(t) + b_1(t)A_t^{(1)}},
\end{aligned} \tag{2.37}$$

where the last equality holds by lemma 2.1. This proves (2.32). The other identities are proven similarly. □

Remark 2.2 Equations (2.32) and (2.34) are similar in nature and appearance. As it is the case for the resulting OIS rate $\{r_t\}$ (2.17), the fact that (2.31) is designed to be a supermartingale has as a consequence that the associated intensity (2.28) is a non-negative process. This is readily seen by observing that $\{\nu_t^{(i)}\}$ is a martingale and thus the drift of the supermartingale (2.31) is given by the necessarily non-negative process $\{\gamma_t^{(i)}\}$ that drives $\{Z_t^{(i)}\}$.

At time $t = 0$, we have $A_0^{(i)} = 0$, hence only the terms $c_i(T)$ remain in these formulas. Since the formulae (2.32) and (2.33) are not affected by the inclusion of the credit component in this approach, the valuation of the basis swap of section 5.2 remains unchanged. By making use of the so-called 'Key Lemma' of credit risk, see for instance Bielecki *et al.* (2009), the identity (2.36) is the main building block for the pre-default

price process of a 'clean' CDS on the counterparty (respectively the bank, substituting τ_b for τ_c in (2.36)). In particular, the identities at $t = 0$

$$\mathbb{E}^{\mathbb{Q}}\left[\mathrm{e}^{-\int_0^T (r_s+\gamma_s^c)\mathrm{d}s}\right] = c_1(T)c_4(T)c_6(T),$$
$$\mathbb{E}^{\mathbb{Q}}\left[\mathrm{e}^{-\int_0^T (r_s+\gamma_s^b)\mathrm{d}s}\right] = c_1(T)c_5(T)c_6(T), \qquad (2.38)$$

for $T \geq 0$, can be applied to calibrate the functions $c_i(T)$, $i = 4, 5, 6$, to CDS curves of the counterparty and the bank, once the dependence on the respective credit risk factors has been specified. The calibration of the 'noisy' credit model components $b_i(T)A_t^{(i)}$, $i = 4, 5, 6$, would require CDS option data or views on CDS option volatilities. If the entire model is judged underdetermined, more parsimonious specifications may be obtained by removing the common default component τ_6 (just letting $\tau_c = \tau_4$, $\tau_b = \tau_5$) and/or restricting oneself to deterministic default intensities by setting some of the stochastic terms equal to zero, i.e. $b_i(T)A_t^{(i)} = 0$, $i = 4, 5$ and/or 6 (as is the case for the one-factor interest rate models in section 3). The core building blocks of our multi-curve LIBOR model with counterparty-risk are the couterparty-risk kernels $\{k_t^{(i)}\}$, $i = 4, 5, 6$, the OIS kernel $\{h_t\}$ and the LIBOR kernel given by the numerator of the LIBOR process (2.26). We may view all kernels as defined under the $\mathbb{M}$-measure, *a priori*. The respective kernels under the $\mathbb{P}$-measure, e.g. the pricing kernel $\{\pi_t\}$, are obtained as explained at the end of section 5.2.

3. Clean valuation

The next questions we address are centred around the pricing of LIBOR derivatives and their calibration to market data, especially LIBOR swaptions, which are the most liquidly traded (non-linear) interest rate derivatives. Since market data typically reflect prices of fully collaterallized transactions, which are funded at a remuneration rate of the collateral that is best proxied by the OIS rate, we consider in this section clean valuation ignoring counterparty-risk for the purpose of model calibration in the next section and thus assume funding at the rate r_t. That is, in this part, we do not make use of the credit-intensity models proposed in section 2.4, but will apply them in section 5 for the computation of counterparty-risk and funding valuation adjustments.

An interest rate swap, see for instance Brigo and Mercurio (2006), is an agreement between two counterparties, where one stream of future interest payments is exchanged for another based on a specified nominal amount N. A popular interest rate swap is the exchange of a fixed rate (contractual swap spread) against the LIBOR at the end of successive time intervals $[T_{i-1}, T_i]$ of length δ. Such a swap can also be viewed as a collection of n FRA. The swap price Sw_t at time $t \leq T_0$ is given by the following model-independent formula:

$$Sw_t = N\delta \sum_{i=1}^{n} [L(t; T_{i-1}, T_i) - K P_{tT_i}].$$

Remark 3.1 In the market, a floating leg has typically higher frequency than a fixed leg. For simplicity, we consider the case when the timings of the fixed and floating payments are the same. Of course, taking different frequencies can be accommodated.

A swaption is an option between two parties to enter a swap at the expiry date T_k (the maturity date of the option). Its price at time $t \leq T_k$ is given by the following $\mathbb{M}$-pricing formula:

$$\begin{aligned} Swn_{tT_k} &= \frac{N\delta}{h_t}\mathbb{E}^{\mathbb{M}}[h_{T_k}(Sw_{T_k})^+|\mathcal{F}_t] \\ &= \frac{N\delta}{h_t}\mathbb{E}^{\mathbb{M}}\left[h_{T_k}\left(\sum_{i=k+1}^{n}[L(T_k; T_{i-1}, T_i) - K P_{T_kT_i}]\right)^+ \Big| \mathcal{F}_t\right] \\ &= \frac{N\delta}{P_{0t} + b_1 A_t^{(1)}}\mathbb{E}^{\mathbb{M}}\Big[\Big(\sum_{i=k+1}^{n}\big[L(0; T_{i-1}, T_i) + b_2(T_{i-1}, T_i) \\ &\qquad \times A_{T_k}^{(2)} + b_3(T_{i-1}, T_i)A_{T_k}^{(3)} \\ &\qquad - K(P_{0T_i} + b_1(T_i)A_{T_k}^{(1)})\big]\Big)^+ \Big| \mathcal{F}_t\Big], \end{aligned} \qquad (3.1)$$

using the formulae (2.22) and (2.26) for $P_{T_kT_i}$ and $L(T_k; T_{i-1}, T_i)$. In particular, the swaption prices at time $t = 0$ can be rewritten by use of $A_t^{(i)} = S_t^{(i)} - 1$ so that

$$\begin{aligned} Swn_{0T_k} &= N\delta\,\mathbb{E}^{\mathbb{M}}\left[\left(c_2 A_{T_k}^{(2)} + c_3 A_{T_k}^{(3)} - c_1 A_{T_k}^{(1)} + c_0\right)^+\right] \\ &= N\delta\,\mathbb{E}^{\mathbb{M}}\left[\left(c_2 S_{T_k}^{(2)} + c_3 S_{T_k}^{(3)} - c_1 S_{T_k}^{(1)} + \tilde{c}_0\right)^+\right], \end{aligned} \qquad (3.2)$$

where

$$c_2 = \sum_{i=k+1}^{n} b_2(T_{i-1}, T_i), \quad c_3 = \sum_{i=k+1}^{n} b_3(T_{i-1}, T_i),$$
$$c_1 = K\sum_{i=k+1}^{n} b_1(T_i),$$
$$c_0 = \sum_{i=k+1}^{n}[L(0; T_{i-1}, T_i) - K P_{0T_i}], \ \tilde{c}_0 = c_0 + c_1 - c_2 - c_3.$$

As we will see in several instances of interest, these expectations can be computed efficiently with high accuracy by various numerical schemes.

Remark 3.2 The advantages of modelling the LIBOR process $\{L(t; T_{i-1}, T_i)\}$ by a rational function of which denominator is the discount factor (pricing kernel) associated with the employed pricing measure (in this case $\mathbb{M}$) are: (i) the rational form of $\{L(t; T_{i-1}, T_i)\}$ and also of $\{P_{tT_i}\}$ produces, when multiplied with the discount factor $\{h_t\}$, a linear expression in the $\mathbb{M}$-martingale drivers $\{A_t^{(i)}\}$. This is in contrast to other akin pricing formulae, in which the factors appear as sums of exponentials, see e.g. Crépey *et al.* (2015), Equation (33). (ii) The dependence structure between the LIBOR process and the OIS discount factor $\{h_t\}$—or the pricing kernel $\{\pi_t\}$ under the $\mathbb{P}$-measure—is clear-cut. The numerator of $\{L(t; T_{i-1}, T_i)\}$ is

driven only by idiosyncratic stochastic factors that influence the dynamics of the LIBOR process. We may call such drivers the 'LIBOR risk factors'. Dependence on the 'OIS risk factors', in our model example $\{A_t^{(1)}\}$, is produced solely by the denominator of the LIBOR process. (iii) Usually, the FRA process $K_t = L(t; T_{i-1}, T_i)/P_{tT_i}$ is modelled directly and more commonly applied to develop multi-curve frameworks. With such models, however, it is not guaranteed that simple pricing formulae like (3.1) can be derived. We think that the 'codebook', (2.6) and (2.26) in the considered example, is more suitable for the development of consistent, flexible and tractable multi-curve models.

We next consider one-factor and two-factor models in preparation for calibration to market data. The ultimate goal is to find a simple, parsimonious and tractable interest rate model that can be accurately calibrated to swaptions written on LIBOR.

3.1. Univariate Fourier pricing

We begin with a much simplified model that is driven by a single market factor. We will eventually see that such a choice is unrealistic and in particular the resulting model is too rigid to allow for satisfactory model calibration. One might justify such a model by saying that since in current markets there are no liquidly traded OIS derivatives, no useful data are available; a pragmatic simplification is to assume deterministic OIS rates $\{r_t\}$. However, this assumption produces unrealistic future scenarios for the basis spreads between OIS and LIBOR rates, which are not guaranteed to be positive. Hence, we shall relax such an assumption later when we consider a two-factor model, and thus OIS returns to be a stochastic process.

Let us assume $A_t^{(1)} = 0$, and hence $b_1(t)$ plays no role either, so that it can be assumed equal to zero. Furthermore, for a start, we assume $A_t^{(3)} = 0$ and $b_3(t) = 0$, and (3.2) simplifies to

$$\begin{aligned} Swn_{0T_k} &= N\delta\,\mathbb{E}^{\mathbb{M}}\left[\left(c_2 A_{T_k}^{(2)} + c_0\right)^+\right] \\ &= N\delta\,\mathbb{E}^{\mathbb{M}}\left[\left(c_2 S_{T_k}^{(2)} + \tilde{c}_0\right)^+\right], \end{aligned}$$

where here $\tilde{c}_0 = c_0 - c_2$. For $\tilde{c}_0 > 0$, the price is simply $Swn_{0T_k} = N\delta c_0$. For $\tilde{c}_0 < 0$, and in the case of an exponential-Lévy martingale model with

$$S_t^{(2)} = \mathrm{e}^{X_t^{(2)} - t\,\psi_2(1)},$$

where $\{X_t^{(2)}\}$ is a Lévy process with cumulant ψ_2 such that

$$\mathbb{E}^{\mathbb{M}}\left[\mathrm{e}^{zX_t^{(2)}}\right] = \exp\left[t\psi_2(z)\right], \tag{3.3}$$

we have

$$Swn_{0T_k} = \frac{N\delta}{2\pi}\int_{\mathbb{R}} \frac{\tilde{c}_0^{\,1-iv-R}\, M_{T_k}^{(2)}(R+iv)}{(R+iv)(R+iv-1)}\mathrm{d}v, \tag{3.4}$$

where

$$M_{T_k}^{(2)}(z) = \mathrm{e}^{T_k\psi_2(z) + z\left(\ln(c_2) - \psi_2(1)\right)}$$

and R is an arbitrary constant ensuring finiteness of $M_{T_k}^{(2)}(R + iv)$ for $v \in \mathbb{R}$. For details concerning (3.4), we refer to Eberlein *et al.* (2010).

3.2. One-factor log-normal model

In the event that $\{A_t^{(1)}\} = \{A_t^{(3)}\} = 0$ and $\{A_t^{(2)}\}$ is of the form

$$A_t^{(2)} = \exp\left(a_2 X_t^{(2)} - \frac{1}{2}a_2^2 t\right) - 1, \tag{3.5}$$

where $\{X_t^{(2)}\}$ is a standard Brownian motion and a_2 is a real constant, it follows from simple calculations that the swaption price is given, for $\tilde{c}_0 = c_0 - c_2$, by

$$\begin{aligned} Swn_{0T_k} &= N\delta\,\mathbb{E}^{\mathbb{M}}\left[\left(c_2 A_{T_k}^{(2)} + c_0\right)^+\right] \qquad (3.6) \\ &= N\delta\left(c_2\Phi\left(\frac{\frac{1}{2}a_2^2 T_k - \ln(-\tilde{c}_0/c_2)}{a_2\sqrt{T_k}}\right)\right. \\ &\quad \left. + \tilde{c}_0\Phi\left(\frac{-\frac{1}{2}a_2^2 T_k - \ln(-\tilde{c}_0/c_2)}{a_2\sqrt{T_k}}\right)\right), \qquad (3.7) \end{aligned}$$

where $\Phi(x)$ is the standard normal distribution function. In section 4, where we focus on model calibration, we also consider a one-factor model that is driven by an NIG-process, as an example of a model with jumps.

3.3. Two-factor log-normal model

We return to the price formula (3.2) and consider the case where the martingales $\{A_t^{(i)}\}$ are given, for $i = 1, 2, 3$, by

$$A_t^{(i)} = \exp\left(a_i X_t^{(i)} - \frac{1}{2}a_i^2 t\right) - 1, \tag{3.8}$$

for real constants a_i and standard Brownian motions $\{X_t^{(1)}\} = \{X_t^{(3)}\}$ and $\{X_t^{(2)}\}$ with correlation ρ. Then, it follows that

$$\begin{aligned} Swn_{0T_k} = \mathbb{E}^{\mathbb{M}}\Big[\Big(&c_2\mathrm{e}^{X\sqrt{T_k}a_2 - \frac{1}{2}a_2^2 T_k} + c_3\mathrm{e}^{Y\sqrt{T_k}a_3 - \frac{1}{2}a_3^2 T_k} \\ &- c_1\mathrm{e}^{Y\sqrt{T_k}a_1 - \frac{1}{2}a_1^2 T_k} + \tilde{c}_0\Big)^+\Big], \end{aligned} \tag{3.9}$$

where $X \sim \mathcal{N}(0,1)$, $Y \sim \mathcal{N}(0,1)$, $(X|Y) = y \sim \mathcal{N}(\rho y, (1-\rho^2))$. Hence,

$$\begin{aligned} &Swn_{0T_k} \\ &= \int_{-\infty}^{\infty}\int_{-\infty}^{\infty}(c_2\mathrm{e}^{x\sqrt{T_k}a_2 - \frac{1}{2}a_2^2 T_k} - K(y))^+ f(x|y)f(y)\mathrm{d}x\mathrm{d}y \\ &= \int_{K(y)>0}\left(\int_{-\infty}^{\infty}(c_2\mathrm{e}^{x\sqrt{T_k}a_2 - \frac{1}{2}a_2^2 T_k} - K(y))^+ f(x|y)\mathrm{d}x\right) f(y)\mathrm{d}y \\ &+ \int_{K(y)<0}\left(\int_{-\infty}^{\infty}(c_2\mathrm{e}^{x\sqrt{T_k}a_2 - \frac{1}{2}a_2^2 T_k} - K(y))^+ f(x|y)\mathrm{d}x\right) f(y)\mathrm{d}y, \end{aligned}$$

where

$$\begin{aligned} K(y) &= c_1(\mathrm{e}^{a_1\sqrt{T_k}y - \frac{1}{2}a_1^2 T_k} - 1) - c_3(\mathrm{e}^{a_3\sqrt{T_k}y - \frac{1}{2}a_3^2 T_k} - 1) - c_0, \\ f(y) &= \frac{1}{\sqrt{2\pi}}\mathrm{e}^{-\frac{y^2}{2}}, \\ f(x|y) &= \frac{1}{\sqrt{2\pi(1-\rho^2)}}\mathrm{e}^{\frac{-(x-\rho y)^2}{2(1-\rho^2)}}. \end{aligned}$$

This expression can be simplified further to obtain

$$
\begin{aligned}
&Swn_{0T_k} \\
&= \int_{K(y)>0} \Bigg[c_2 \mathrm{e}^{a_2\sqrt{T_k}\,\rho y + \frac{1}{2}a_2^2 T_k(1-\rho^2)}\Phi \\
&\quad \times \left(\frac{\rho y + a_2\sqrt{T_k}(1-\rho^2) + \ln(c_2) - \frac{1}{2}a_2^2 T_k - K(y)}{\sqrt{1-\rho^2}} \right) \\
&\quad - K(y)\Phi\left(\frac{\rho y + \ln(c_2) - \frac{1}{2}a_2^2 T_k - K(y)}{\sqrt{1-\rho^2}} \right) \Bigg] f(y)\mathrm{d}y \\
&\quad + \int_{K(y)<0} \left(c_2 \mathrm{e}^{a_2\sqrt{T_k}\rho(y - \frac{1}{2}a_2\sqrt{T_k}\rho} - K(y) \right) f(y)\mathrm{d}y.
\end{aligned}
$$

The calculation of the swaption price is then reduced to calculate two one-dimensional integrals. Since the regions of integration are not explicitly known, one has to numerically solve for the roots of $K(y)$, which may have up to two roots. Nevertheless, a full swaption smile can be calculated in a small fraction of a second by means of this formula.

4. Calibration

The counterparty-risk valuation adjustments, abbreviated by XVAs (credit valuation adjustment (CVA), debt valuation adjustment (DVA), etc.), can be viewed as long-term options on the underlying contracts. For their computation, the effects by the volatility smile and term structure matter. Furthermore, for the planned XVA computations of multi-curve products (e.g. basis swaps), which we shall consider in the next section, it is necessary to calibrate the proposed pricing model to financial instruments with underlying tenors of $\delta = 3m$ and $\delta = 6m$. Similar to Crépey *et al.* (2015), we make use of the following EUR market Bloomberg data of 4 January 2011 to calibrate our model: EONIA, three-month EURIBOR and six-month EURIBOR initial term structures, on the one hand, and three-month and six-month tenor swaptions, on the other. As in the HJM framework of Crépey *et al.* (2015), to which the reader is referred for more details in this regard, the initial term structures are fitted by construction in our set-up. With regard to the calibration to swaptions, at first, we calibrate the non-maturity/tenor-dependent parameters to the swaption smile for the 9Y1Y swaption with a three-month tenor underlying. The market smile corresponds to a vector of strike bps $[-200, -100, -50, -25, 0, 25, 50, 100, 200]$ around the underlying forward swap spread. Then, we make use of at-the-money swaptions on 3- and 6-month tenor swaps, all terminating at exactly 10 years, but with maturities from 1 to 9 years. This co-terminal procedure is chosen with a view towards the XVA application in section 5, where a basis swap with a 10-year terminal date is considered.

The general idea leading through section 4 is that we calibrate the 'simplest' stochastic interest rate model, driven by one factor, where two cases are considered: (i) log-normal factor and (ii) log-NIG factor. It turns out that neither of these models calibrates to swaption data satisfactorily, thus suggesting that a two-factor rational model is the next class that needs to be taken under consideration. As we will find out, the two-factor rational log-normal multi-curve interest rate model provides good calibration properties and is deemed to be the 'winning' model. Another conclusion is that we do not need to include jump drivers in the specification of the two-factor rational model.

Model calibration in a one-factor set-up where, say, $\{A_t^{(2)}\}$ is the single stochastic factor, involves the following steps:

(1) We calibrate the parameters of the driving martingale $\{A_t^{(2)}\}$ to the smile of the 9Y1Y swaption with tenor $\delta = 3m$. This part of the calibration procedure gives us also the values of $b_2(9, 9.25)$, $b_2(9.25, 9.5)$, $b_2(9.5, 9.75)$ and $b_2(9.75, 10)$, which we assume to be equal.

(2) Next, we consider the co-terminal, ΔY$(10-\Delta)$Y ATM swaptions with $\Delta = 1, 2, \ldots, 9$ years. These are available written on the three- and six-month rates. We calibrate the remaining values of b_2 one maturity at a time, going backwards and starting with the 8Y2Y for the three-month tenor and with the 9Y1Y for the six-month tenor. This is done assuming that the parameters are piecewise constant, such that $b_2(T, T+0.25) = b_2(T+0.25, T+0.5) = b_2(T+0.5, T+0.75) = b_2(T+0.75, T+1)$ for each $T = 0, 1, \ldots, 8$.

4.1. *One-factor log-normal model*

In the one-factor log-normal specification of section 3.2, we calibrate the parameter a_2 and $b = b_2(9, 9.25) = b_2(9.25, 9.5) = b_2(9.5, 9.75) = b_2(9.75, 10)$ with Matlab utilizing the procedure 'lsqnonlin' based on the pricing formula (3.6) (if $\tilde{c}_0 < 0$, otherwise $Swn_{0T_k} = N\delta c_0$). This calibration yields:

$$a_2 = 0.0537, \quad b = 0.1107.$$

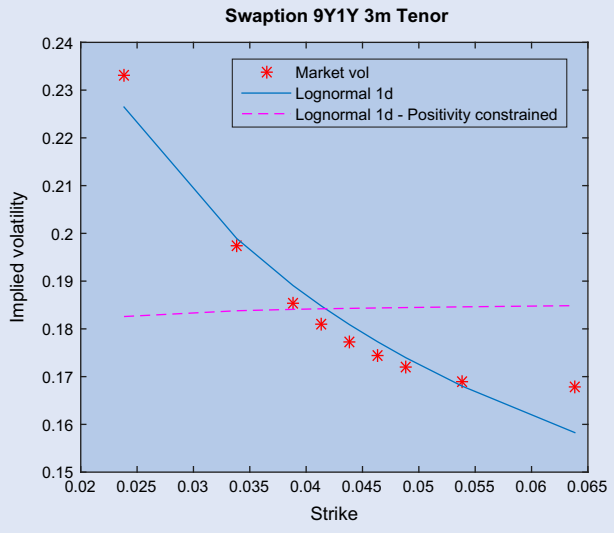

Figure 1. Log-normal one-factor calibration.

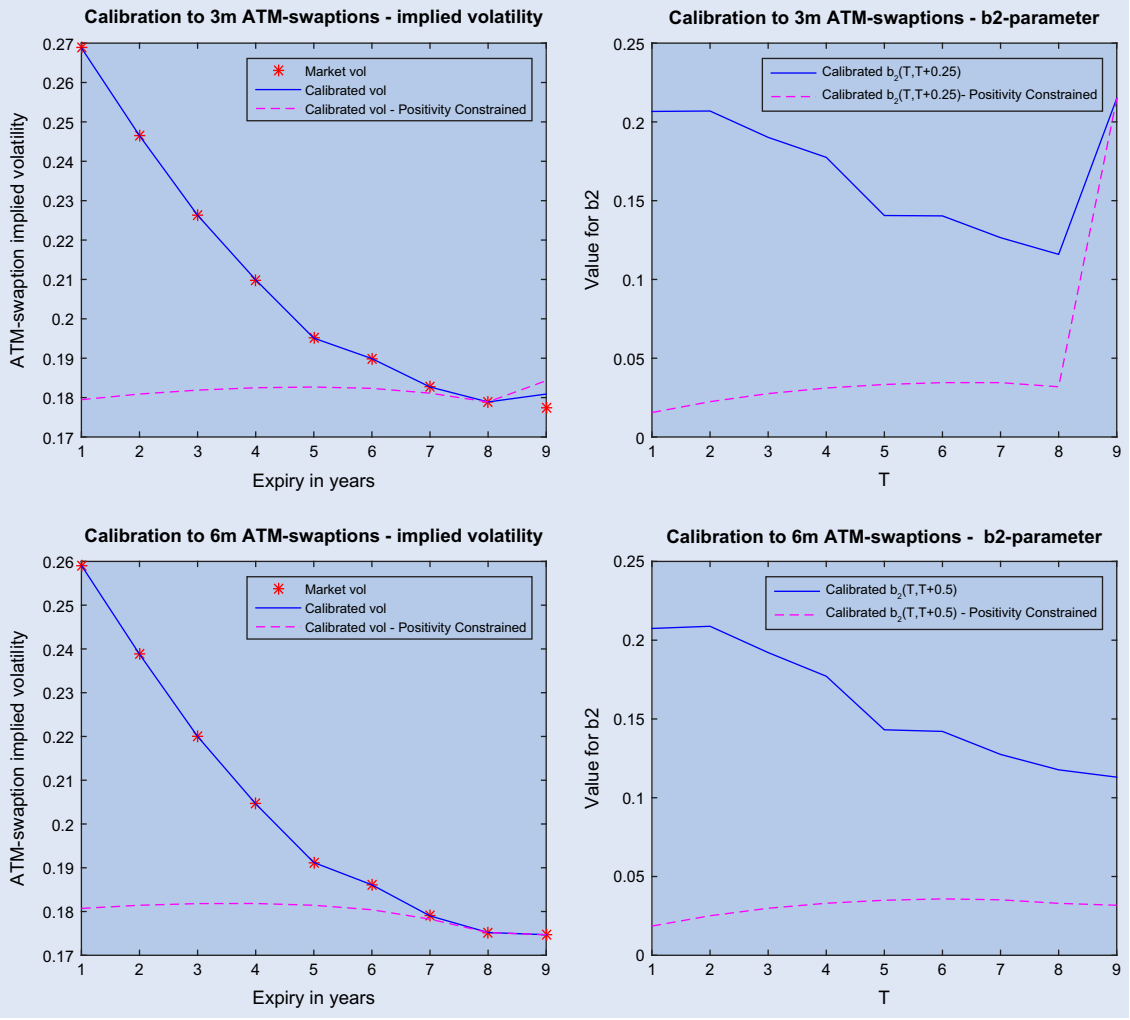

Figure 2. One-factor log-normal calibration. *(Left)* Fit to ATM swaption implied volatility term structures. *(Right)* Calibrated values of the b_2 parameters. *(Top)* $\delta = 3m$. *(Bottom)* $\delta = 6m$.

Forcing positivity of the underlying LIBOR rates means, in this particular case, restricting $b \leq L(0; 9.75, 10) = 0.0328$, c.f. (2.27). The constrained calibration yields:

$$a_2 = 0.1864, \quad b = 0.0328.$$

The two resulting smiles can be found in figure 1, where we can see that the unconstrained model achieves a reasonably good calibration. However, enforcing positivity is highly restrictive since the Gaussian model, in this setting, cannot produce a downward sloping smile.

Next, we calibrate the b_2 parameters to the ATM swaption term structures of three-month and six-month tenors. The results are shown in figure 2. When positivity is not enforced, the model can be calibrated with no error to the market quotes of the ATM co-terminal swaptions. However, one can see from the figure that the positivity constraint does not allow the b_2 function to take the necessary values, and thus a very poor fit to the data is obtained, in particular for shorter maturities.

With this in mind, the natural question is whether the positivity constraint is too restrictive. Informal discussions with market participants reveal that positive probability for negative rates is not such a critical issue for a model. As long as the probability mass for negative values is not substantial, it is a feature that can be lived with. Indeed, assigning a small probability to this event may even be realistic.† In order to investigate the significance of the negative rates and spreads issue mentioned in remark 2.1, we calculate lower quantiles for spot rates as well as the spot spread for the model calibrated without the positivity constraint. As figure 3 shows, the lower quantiles for the rates are of no concern. Indeed, it can hardly be considered pathological that rates will be below -14 basis points with 1% probability on a three-year time horizon. Similarly, with regard to the spot spread, the lower quantile is in fact positive for all time horizons. Further calculations reveal that the probabilities of the eight-year spot spread being negative is 1.1×10^{-5} and the nine year is 0.008—which again can hardly be deemed pathologically high.

We find that the model performs surprisingly well, despite the parsimony of a one-factor log-normal set-up. While positiv-

†A broad panel of money market rates are currently negative, including DKK (CIBOR), short-term EURIBOR and CHF LIBOR.

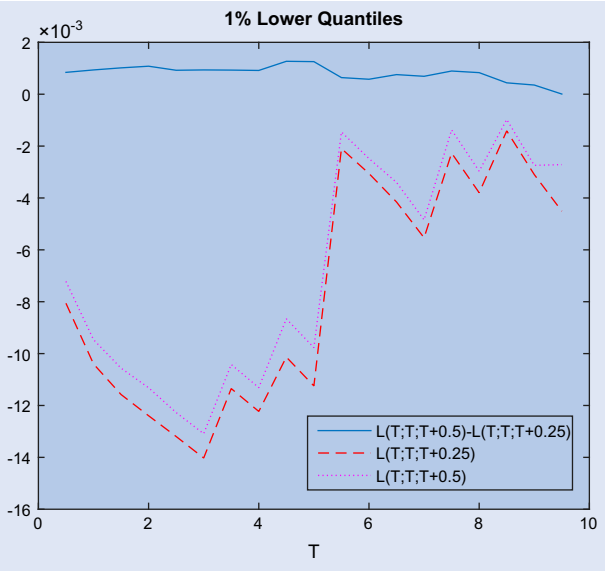

Figure 3. One-Factor log-normal calibration. 1% lower quantiles.

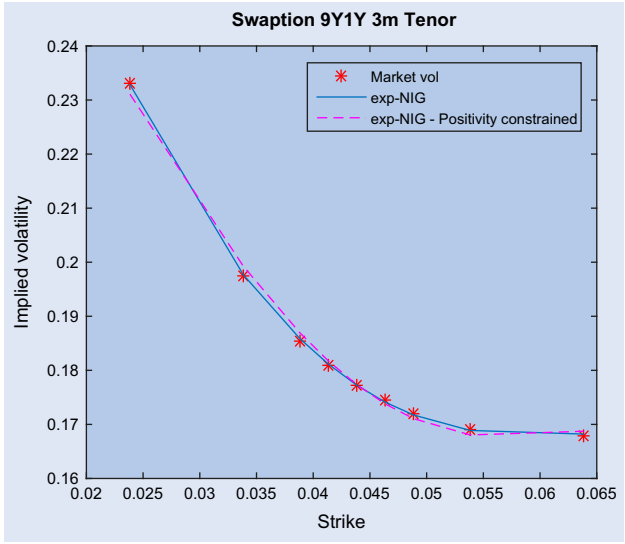

Figure 4. Exponential-NIG calibration.

ity of rates and spreads are not achieved, the model assigns only small probabilities to negative values. However, the ability of fitting the smile with such a parsimonious model is not satisfactory (cf. figure 1), which is our motivation for the next specification.

4.2. *Exponential normal inverse Gaussian model*

The one-factor model, which is driven by a Gaussian factor $\{A_t^{(2)}\}$, is able to capture the level of the volatility smile. Nevertheless, the model-implied skew is slightly different from the market skew. To overcome this issue, we now consider a one-factor model driven by a richer family of Lévy processes. The process $\{A_t^{(2)}\}$ is now assumed to be the exponential normal inverse Gaussian (NIG) $\mathbb{M}$-martingale

$$A_t^{(2)} = \exp\left(X_t^{(2)} - t\psi(1)\right) - 1, \tag{4.1}$$

where $\{X_t^{(2)}\}$ is an $\mathbb{M}$-NIG-process with cumulant $\psi(z)$, see (3.3), expressed in terms of the parametrization† (ν, θ, σ) from Cont and Tankov (2003) as

$$\psi(z) = -\nu\left(\sqrt{\nu^2 - 2z\theta - z^2\sigma^2} - \nu\right), \tag{4.2}$$

where $\nu, \sigma > 0$ and $\theta \in \mathbb{R}$. The parameters that need to be calibrated at first are ν, θ, σ and $b = b_2(9, 9.25) = b_2(9.25, 9.5) = b_2(9.5, 9.75) = b_2(9.75, 10)$. After the calibration, we obtain

$$b = 0.0431, \quad \nu = 0.2498, \quad \theta = -0.0242, \quad \sigma = 0.1584.$$

†The Barndorff-Nielsen (1997) parametrization is recovered by setting $\mu = 0, \alpha = \frac{1}{\sigma}\sqrt{\frac{\theta_i^2}{\sigma_i^2} + \nu_i^2}$, $\beta = \frac{\theta_i}{\sigma_i^2}$ and $\delta = \sigma\nu$.

Imposing $b \leq L(0; 9.75, 10) = 0.0328$ to get positive rates, we obtain instead

$$b = 0.0291, \quad \nu = 0.1354, \quad \theta = -0.0802, \quad \sigma = 0.3048.$$

The two fits are plotted in figure 4. Here, imposing positivity comes at a much smaller cost when compared to the one-factor Gaussian case. The NIG process has a richer structure (more parametric freedom) and therefore is able to compensate for an imposed smaller level of the parameter b_2.

We continue with the second part of the calibration of which results are found in figure 5. Here, we see that enforcing positivity may have a small effect on the smile, but it means that the volatility structure cannot be made to match swaptions with maturity smaller than seven years. Thus, enforcing positivity in this model produces limitations which we wish to avoid. In figure 6, we plot lower quantiles for the rates and spreads as for the one-factor log-normal model. While spot spreads remain positive, the levels do not, and, as shown, the model assigns an unrealistically high probability mass to negative values. In fact, the model assigns a 1% probability to rates falling below -12% within two years! Thus, the one-factor exponential-NIG model loses much of its appeal because it cannot fit long-term smiles and shorter-term ATM volatilities while maintaining realistic values for the interest rate.

4.3. *Calibration of a two-factor log-normal model*

The necessity to produce a better fit to the smile than what can be achieved with the one-factor Gaussian model, while maintaining realistically positive rates and spreads, leads us to proposing the two-factor specification presented in section 3.3. This model is heavily parametrized and the parameters at hand are not all identified by the considered data. We therefore fix the following parameters:

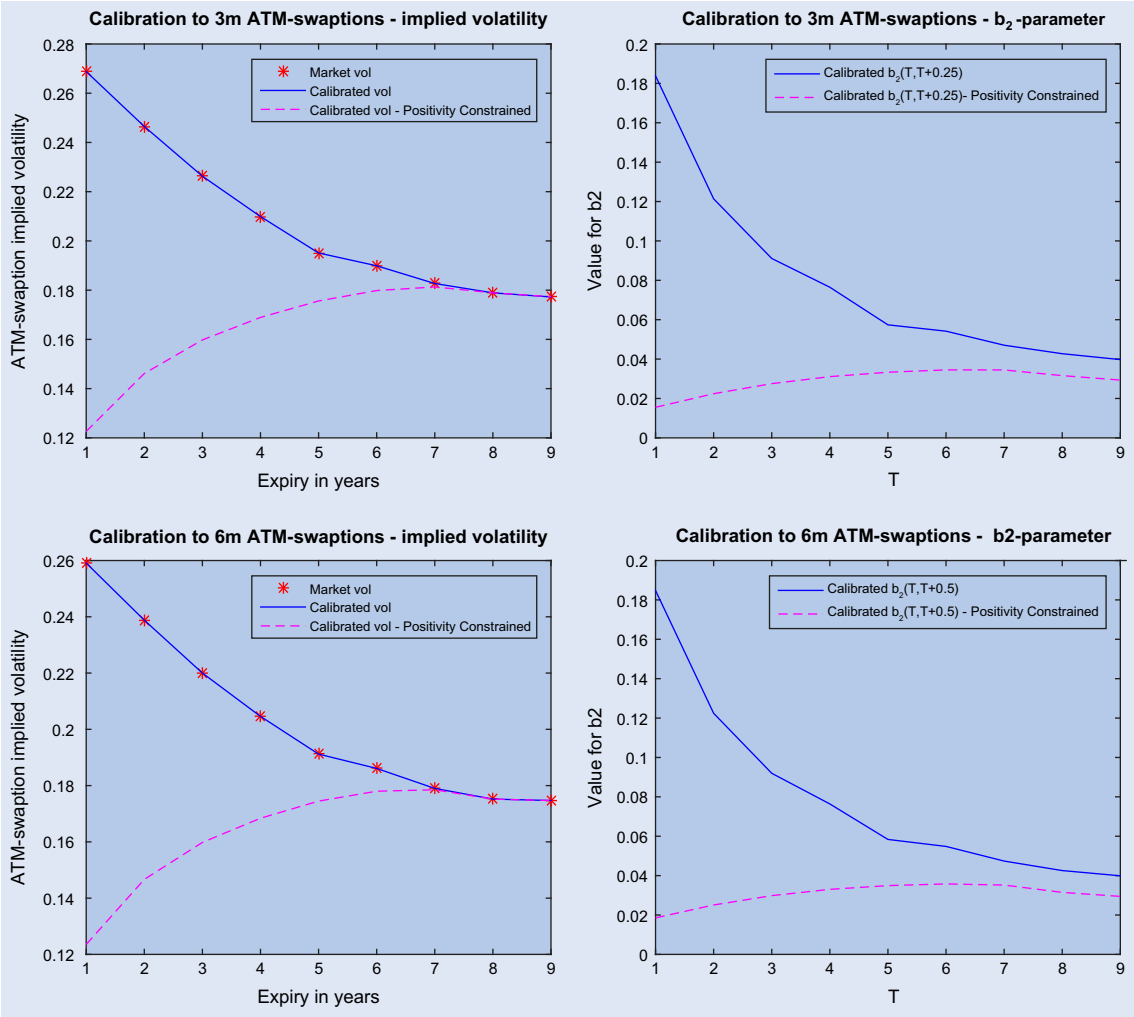

Figure 5. Exponential-NIG calibration. *(Left)* Fit to ATM swaption implied volatility term structures. *(Right)* Calibrated values of the b_2 parameters. *(Top)* $\delta = 3m$. *(Bottom)* $\delta = 6m$.

$$a_1 = 1, \quad a_3 = 1.6, \tag{4.3}$$

$$b_3(T, T+0.25) = 0.15L(0; T; T+0.25), \quad T \in [9, 9.75], \tag{4.4}$$

$$b_2(T, T+0.25) = 0.55L(0, T; T+0.25), \quad T \in [0, 8.75]. \tag{4.5}$$

We assume that b_1 is constant, i.e. $b_1 = b_1(T)$ for $T \in [0, 10]$ and that b_3, outside of the region defined above is piecewise constant, such that $b_3(T, T+0.25) = b_3(T+0.25, T+0.5) = b_3(T+0.5, T+0.75) = b_3(T+0.75, T+1)$ for each $T = 0, 1 \ldots, 8$ and $b_3(T, T+0.5) = b_3(T+0.5, T+1)$ holds for each $T = 0, 1 \ldots, 9$. We furthermore assume that $b_2(T, T+0.5) = b_2(T, T+0.25), \quad T \in [0, 9.5]$. These somewhat *ad hoc* choices are made with a view towards b_2 and b_3 being fairly smooth functions of time. We herewith apply a slightly altered procedure to calibrate the remaining parameters if compared to the scheme utilized for the one-factor models.

(1) We first calibrate to the smile of the 9Y1Y years swaption which gives us the parameters a_2, ρ, the assumed constant value of b_1 and $b_2(9, 9.25)$ to $b_2(9.75, 10)$ which are assumed equal to a constant b. Similar to the exponential-NIG model, we make use of four parameters in total to fit the smile.

(2) The remaining b_2 parameters are determined *a priori*, so what remains is to calibrate the values of b_3. The three-month tenor values $b_3(T, T+0.25)$ for $T \in [0, 8.75]$ are calibrated to ATM, co-terminal swaptions starting from the 8Y2Y years and then continuing backwards to the 1Y9Y instruments. For the six-month tenor products, we calibrate $b_3(T, T+0.5)$ for $T \in [0, 9.5]$, starting with 9Y1Y and proceed backwards.

These are the values we obtain from the first calibration phase: $b_1 = 0.2434, \quad b = 0.02, \quad a_2 = 0.1888, \quad \rho = 0.9530$. The corresponding fit is plotted in the upper left quadrant of figure 7. In order to check the robustness of the calibrated fit through time, we also calibrate to three alternative dates. The quality of the fit appears quite satisfactory and comparable to the exponential-NIG model. For all four dates, the calibration is done enforcing the positivity condition $b_2(T, T+0.25) + b_3(T, T+0.25) \leq L(0; T, T+0.25)$. However, the proce-

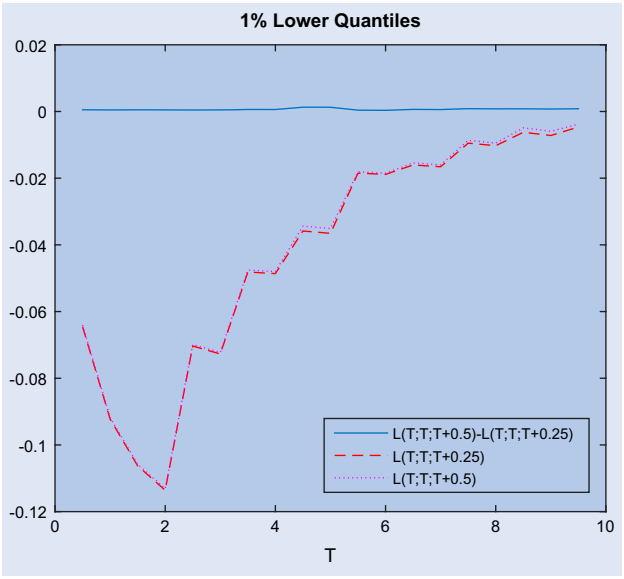

Figure 6. Exponential-NIG calibration calibration. 1% lower quantiles.

dure yields the exact same parameters even if the constraint is relaxed. We thus conclude that a better calibration appears not to be possible for these data-sets by allowing negative rates. Note that it is only for our first data-set that the calibrated correlation ρ is as high as 0.9530. In the other three cases, we have $\rho = 0.4118$, $\rho = 0.3964$ and $\rho = 0.2461$. Figure 8 shows the parameters b_2 and b_3 obtained at the second phase of the calibration to the data of 4 January 2011. As with the previous model (cf. the left graphs of Figures 2 and 5), the volatilities are matched to market data without any error.

We add here that, although not visible from the graphs, the calibrated parameters satisfy the LIBOR spread positivity discussed in remark 2.1.

In conclusion, we find that the two-factor log-normal has the ability to fit the swaption smile very well, it can be controlled to generate positive rates and positive spreads and it is tractable with numerically efficient closed-form expressions for the swaption prices. Given these desirable properties, we discard the one-factor models and retain the two-factor log-normal model for all the analyses in the remaining part of the paper.

5. XVA analysis

So far we have focused on the so-called 'clean computations', i.e. ignoring counterparty-risk and assuming that funding is obtained at the risk-free OIS rate. In reality, contractually specified counterparties at the end of a financial agreement are default and funding to enter or honour a financial agreement may come at a higher cost than at OIS rate. Thus, various valuation adjustments need to be included in the pricing of a financial position. The price of a counterparty-risky financial contract is computed as the difference between the clean price, as in previous sections, and adjustments accounting for counterparty-risk and funding costs, such as CVA, DVA and liquidity-funding valuation adjustment (LVA).

5.1. XVA BSDE

In the reduced-form counterparty-risk set-up of section 2.4, following Crépey (2012), given a contract (or portfolio of contracts) with 'clean' price process $\{P_t\}$ and a time horizon T, the total valuation adjustment (TVA) process $\{\Theta_t\}$ accounting for counterparty-risk and funding cost can be modelled as a solution to an equation of the form

$$\Theta_t = \mathbb{E}_t^{\mathbb{Q}}\left[\int_t^T \exp\left(-\int_t^s (r_u + \gamma_u)\mathrm{d}u\right) f_s(\Theta_s)\mathrm{d}s\right] \quad t \in [0, T], \tag{5.1}$$

for some coefficient $\{f_t(\vartheta)\}$. We note that (5.1) is a backward stochastic differential equation (BSDE) for the TVA process $\{\Theta_t\}$. For accounts on BSDEs and their use in mathematical finance, in general, and counterparty-risk, in particular, we refer to, e.g. El Karoui *et al.* (1997), Brigo *et al.* (2013) and Crépey (2012) or (Crépey *et al.* 2014, Part III). An analysis in line with Crépey (2012) yields a coefficient of the BSDE (5.1) given, for $\vartheta \in \mathbb{R}$, by:

$$\begin{aligned} f_t(\vartheta) &= \underbrace{\gamma_t^c\,(1 - R_c)(P_t - \Gamma_t)^+}_{\mathrm{CVAcoefficient}(cva_t)} - \underbrace{\gamma_t^b(1 - R_b)(P_t - \Gamma_t)^-}_{\mathrm{DVAcoefficient}(dva_t)} \\ &+ \underbrace{\bar{b}_t\Gamma_t^+ - b_t\Gamma_t^- + \tilde{\lambda}_t\big(P_t - \vartheta - \Gamma_t\big)^+ - \lambda_t\big(P_t - \vartheta - \Gamma_t\big)^-}_{\mathrm{LVAcoefficient}(lva_t(\vartheta))}, \end{aligned} \tag{5.2}$$

where:

- R_b and R_c are the recovery rates of the bank towards the counterparty and vice versa.
- $\Gamma_t = \Gamma_t^+ - \Gamma_t^-$, where $\{\Gamma_t^+\}$ (resp. $\{\Gamma_t^-\}$) denotes the value process of the collateral posted by the counterparty to the bank (resp. by the bank to the counterparty), for instance, $\Gamma_t = 0$ (used henceforth unless otherwise stated) or $\Gamma_t = P_t$.
- The processes $\{\bar{b}_t\}$ and $\{b_t\}$ are the spreads with respect to the OIS short rate $\{r_t\}$ for the remuneration of the collateral $\{\Gamma_t^+\}$ and $\{\Gamma_t^-\}$ posted by the counterparty and the bank to each other.
- The process $\{\lambda_t\}$ (resp. $\{\tilde{\lambda}_t\}$) is the liquidity-funding (resp. investment) spread of the bank with respect to $\{r_t\}$. By liquidity-funding spreads we mean that these are free of credit risk. In particular,

$$\tilde{\lambda}_t = \bar{\lambda}_t - \gamma_t^b(1 - \bar{R}_b), \tag{5.3}$$

where $\{\bar{\lambda}_t\}$ is the all-inclusive funding borrowing spread of the bank and where $\bar{R}_b$ stands for a recovery rate of the bank to its unsecured lender (which is assumed risk-free, for simplicity, so that in the case of $\{\lambda_t\}$, there is no credit risk involved in any case).

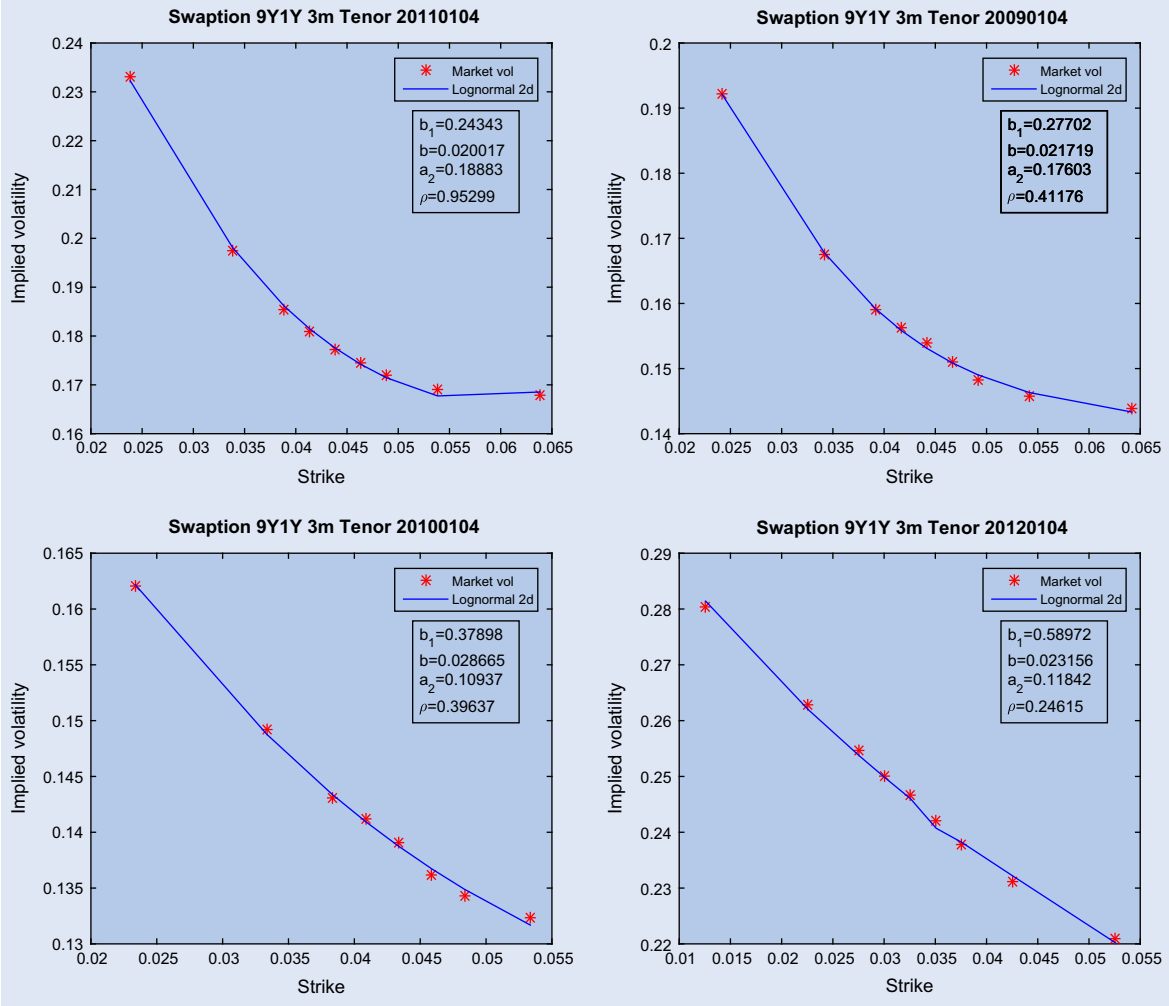

Figure 7. Log-normal two-factor calibration.

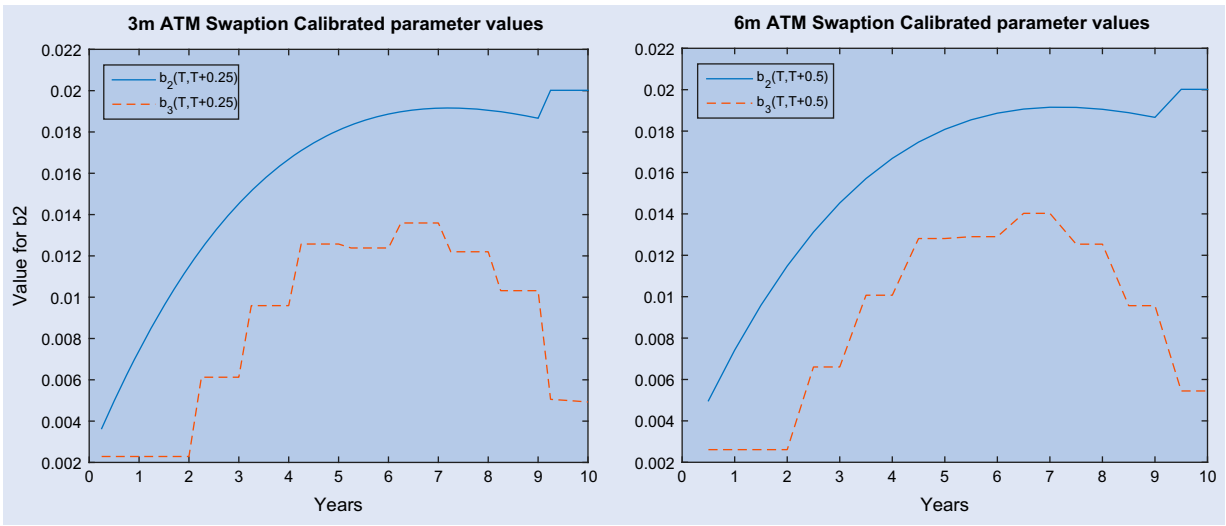

Figure 8. Two-factor log-normal calibration. *(Left)* Parameter values fitted to three-month ATM swaption implied volatility term structures. *(Right)* Parameter values fitted to six-month ATM swaption implied volatility term structures.

The data $\{\Gamma_t\}$, $\{b_t\}$ and $\bar{b}_t$ are specified in a credit support annex (CSA) contracted between the two parties. We note that

$$\mathbb{E}_t^{\mathbb{Q}}\left[\int_t^T \exp\left(-\int_t^s (r_u+\gamma_u)\mathrm{d}u\right) f_s(\Theta_s)\mathrm{d}s\right]$$

$$= \mathbb{E}_t^{\mathbb{M}}\left[\int_t^T \frac{\mu_s \nu_s D_s Z_s}{\mu_s \nu_t D_t Z_t} f_s(\Theta_s)\mathrm{d}s\right]$$
$$= \mathbb{E}_t^{\mathbb{M}}\left[\int_t^T \frac{h_s k_s}{h_t k_t} f_s(\Theta_s)\mathrm{d}s\right]. \tag{5.4}$$

Hence, by setting $\widetilde{\Theta}_t = h_t\, k_t\, \Theta_t$, one obtains the following equivalent formulation of (5.1) and (5.2) under $\mathbb{M}$:

$$\widetilde{\Theta}_t = \mathbb{E}_t^{\mathbb{M}}\left[\int_t^T \tilde{f}_s(\widetilde{\Theta}_s)\mathrm{d}s\right] \quad t \in [0, T], \tag{5.5}$$

where

$$\begin{aligned}\frac{\tilde{f}_t(\tilde{\vartheta})}{h_t k_t} &= f_t\left(\frac{\tilde{\vartheta}}{h_t k_t}\right)\\ &= \gamma_t^c\ (1 - R_c)(P_t - \Gamma_t)^+ - \gamma_t^b(1 - R_b)(P_t - \Gamma_t)^-\\ &\quad + \bar{b}_t\Gamma_t^+ - b_t\Gamma_t^- + \tilde{\lambda}_t\left(P_t - \frac{\tilde{\vartheta}}{h_t k_t} - \Gamma_t\right)^+\\ &\quad - \lambda_t\left(P_t - \frac{\tilde{\vartheta}}{h_t k_t} - \Gamma_t\right)^-. \end{aligned}\tag{5.6}$$

For the numerical implementations presented in the following section, unless stated otherwise, we set:

$$\begin{aligned}&\gamma^b = 5\%,\ \gamma^c = 7\%,\ \gamma = 10\%,\\ &R_b = R_c = 40\%,\\ &b = \bar{b} = \lambda = \tilde{\lambda} = 1.5\%.\end{aligned}\tag{5.7}$$

In the simulation grid, one time step corresponds to one month and $m = 10^4$ or 10^5 scenarios are produced. We recall the comments made after (2.38) and note that (i) the counterparty and the bank may default jointly, which is reflected by the fact that $\gamma_t < \gamma_t^b + \gamma_t^c$, and (ii) we consider a case where default intensities are assumed deterministic, that is, $b_i A^{(i)} = 0$ ($i = 4, 5, 6$). In fact, any stochasticity of the default intensities $\{\gamma_t^{(i)}\}$ would be averaged out in all the pricing formulae at $t = 0$ that are derived below (but it would appear in more general t-pricing formulae or in the XVA greeks even for $t = 0$).

5.2. *Basis swap case study*

A typical multi-curve financial product, i.e. one that significantly manifests the difference between single-curve and multi-curve discounting, is the so-called basis swap. Such an instrument consists of exchanging two streams of floating payments based on a nominal cash amount N or, more generally, a floating leg against another floating leg plus a fixed leg. In the classical single-curve set-up, the value of a basis swap (without fixed leg) is zero throughout its life. Since the onset of the financial crisis in 2007, markets quote positive basis swap spreads that have to be added to the smaller tenor leg, which is clear evidence that LIBOR is no longer accepted as an interest rate free of credit and liquidity risk. We consider a basis swap with a duration of 10 years where payments based on LIBOR of 6-month tenor are exchanged against payments based on LIBOR of 3-month tenor plus a fixed spread. The two payment streams start and end at the same time $T_0 = T_0^1 = T_0^2$, $T = T_{n_1}^1 = T_{n_2}^2$. The value at time t of the basis swap with spread K is given, for $t \le T_0$, by

$$BS_t = N\Bigg(\sum_{i=1}^{n_1}\delta_i^{6m} L(t; T_{i-1}^1, T_i^1) - \sum_{j=1}^{n_2}\delta_j^{3m}\left(L(t; T_{j-1}^2, T_j^2) + K P_{tT_j^2}\right)\Bigg).$$

After the swap has begun, i.e. for $T_0 \le t < T$, the value is given by

$$\begin{aligned}BS_t = N\Bigg(&\delta_{i_t}^{6m} L(T_{i_t-1}^1; T_{i_t-1}^1, T_{i_t}^1) + \sum_{i=i_t+1}^{n_1}\delta_i^{6m} L(t; T_{i-1}^1, T_i^1)\\ &- \delta_{j_t}^{3m}\left(L(T_{j_t-1}^2; T_{j_t-1}^2, T_{j_t}^2) + K P_{tT_{j_t}^2}\right)\\ &- \sum_{j=j_t+1}^{n_2}\delta_j^{3m}\left(L(t; T_{j-1}^2, T_j^2) + K P_{tT_j^2}\right)\Bigg),\end{aligned}$$

where $T_{i_t}^1$ (respectively, $T_{j_t}^2$) denotes the smallest T_i^1 (respectively, T_i^2) that is strictly greater than t. The spread K is chosen to be the fair basis swap spread at T_0 so that the basis swap has value zero at inception. We have

$$K = \frac{\sum_{i=1}^{n_1}\delta_i^{6m} L(T_0; T_{i-1}^1, T_i^1) - \sum_{j=1}^{n_2}\delta_j^{3m} L(T_0; T_{j-1}^2, T_j^2)}{\sum_{j=1}^{n_2}\delta_j^{3m} P_{T_0 T_j^2}}.$$

The price processes on which the numerical illustration in figure 9 has been obtained were simulated by applying the calibrated two-factor log-normal model developed in section 4.3. The basis swap is assumed to have a notional cash amount $N = 100$ and maturity $T = 10$ years. In the two-factor log-normal set-up, the basis swap spread at time $t = 0$ is $K = 12$ basis points, which is added to the three-month leg so that the basis swap is incepted at par. The $t = 0$ value of both legs is then equal to EUR 27.96. The resulting risk exposure, in the sense of the expectation and quantiles of the corresponding price process at each point in time, is shown in the left graphs of figure 9, where the right plots correspond to the $\mathbb{P}$-exposure discussed below. Due to the discrete coupon payments, there are two distinct patterns of the price process exposure, most clearly visible at times preceding payments of the six-month tenor coupons for the first one and at times preceding payments of the three-month tenor coupons without the payments of the six-month tenor coupons for the second one. We show the exposures at such respective dates on the upper and lower plots in figure 9.

5.2.1. Lévy random bridges. The basis swap exposures in figure 9 are computed under the auxiliary $\mathbb{M}$-measure. The XVAs that are computed in later sections are derived from these $\mathbb{M}$-exposures. However, exposures are also needed for risk management and as such need to be evaluated under the real-world measure $\mathbb{P}$. This means that a measure change from $\mathbb{M}$ to $\mathbb{P}$ needs to be defined, which requires some thoughts as to what features of a price dynamics under $\mathbb{P}$ one might like to capture through a specific type of measure change and hence

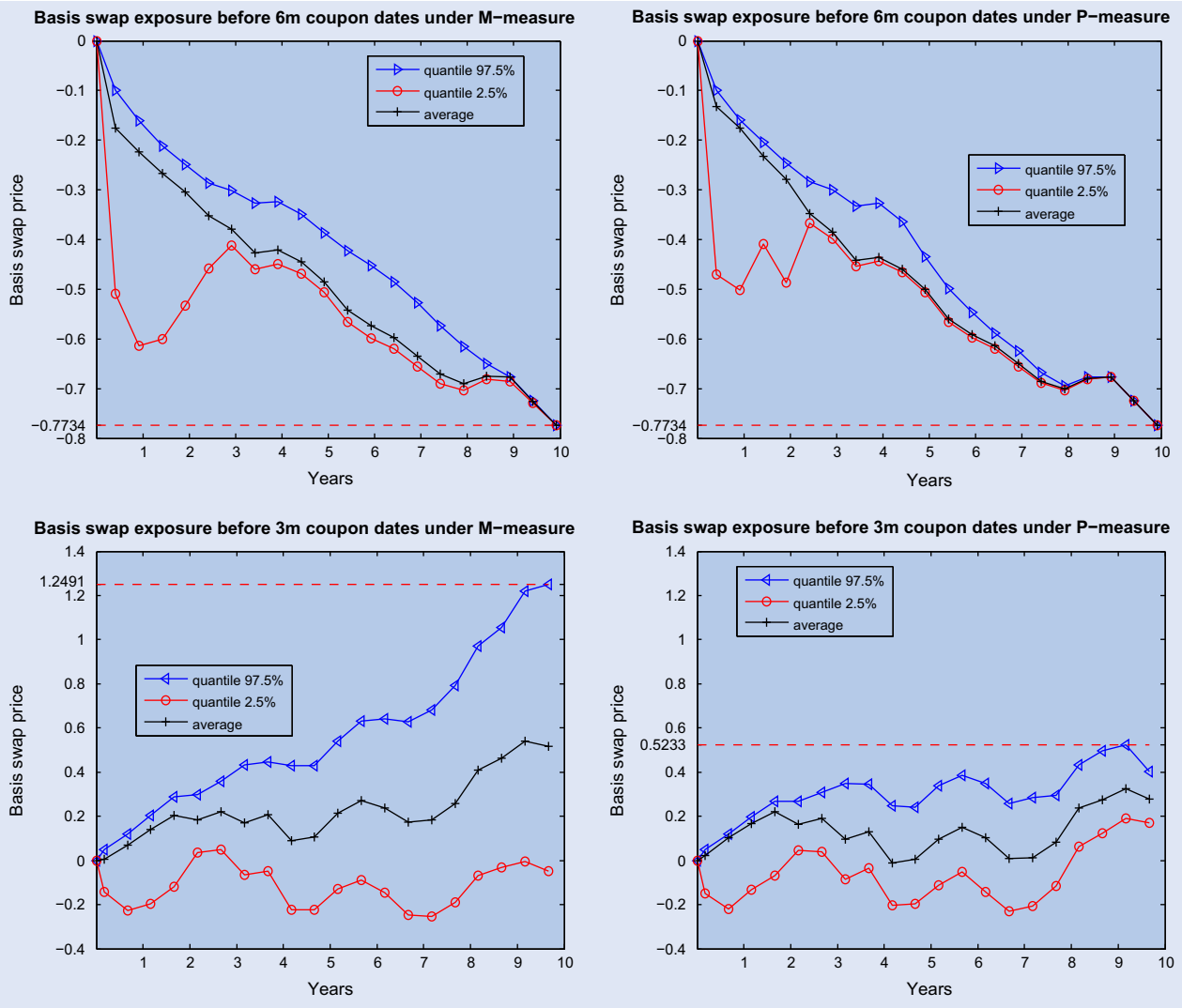

Figure 9. Exposures of a basis swap (price process with mean and quantiles) in the calibrated two-factor Gaussian model. *(Top)* Exposure of the basis swap at $t = 5m, 11m, etc.$ *(Bottom)* Exposure of the basis swap price at $t = 2m, 8m, 14m, etc.$ *(Left)* Exposure under the $\mathbb{M}$-measure. *(Right)* Exposure under the $\mathbb{P}$-measure with the prediction that the LIBOR rate $L(10.75y; 10.75y, 11y)$ will be either 2 % with probability $p = 0.7$ or 5 % with probability $1 - p = 0.3$.

by the induced $\mathbb{P}$-model. In other words, we design a measure change so as to induce a particular stochastic behaviour of the $\{A_t\}$ processes under $\mathbb{P}$, and in particular of the underlying Markov processes $\{X_t\}$ driving them.

A special case we consider in what follows is where $\{X_t\}$ is a Lévy process under $\mathbb{M}$, while it adopts the law of a corresponding (possibly multivariate, componentwise) Lévy random bridge (LRB) under $\mathbb{P}$. Several explicit asset price models driven by LRBs have been developed in Macrina (2014). The LRB-driven rational pricing models have a finite time horizon. The LRB is characterized, apart from the type of underlying Lévy process, by the terminal $\mathbb{P}$-marginal distribution to which it is pinned at a fixed time horizon U. The terminal distribution can be arbitrarily chosen, but its specification influences the behaviour of the LRB as time approaches U. In turn, the properties of a specified LRB influence the behaviour of $\{A_t\}$ and hence the dynamics of the considered price process. We see an advantage in having the freedom of specifying the $\mathbb{P}$-distribution of the factor process at some fixed future date. This way, we can implement experts' opinions (e.g. personal beliefs based on some expert analysis) in the $\mathbb{P}$-dynamics of the price process as to what level, say, an interest rate (e.g. OIS, LIBOR) is likely to be centred around at a fixed future date.

The recipe for the construction of an LRB can be found in Hoyle *et al.* (2011), Definition 3.1, which is extended for the development of a multivariate LRB in Macrina (2014). LRBs have the property, as shown in Proposition 3.7 of Hoyle *et al.* (2011), that there exists a measure change to an auxiliary measure with respect to which the LRB has the law of the constituting Lévy process. That is, we suppose the auxiliary measure is $\mathbb{M}$ and we have an LRB $\{X_t\}_{0\leq t\leq U}$ defined on the finite time interval $[0, U]$ where U is fixed. Under $\mathbb{M}$ and on $[0, U)$, $\{X_t\}$ has the law of the underlying Lévy process. To illustrate further, let us assume a univariate LRB; the analogous

measure change for multivariate LRBs is given in Macrina (2014). Under $\mathbb{P}$, which stands in relation with $\mathbb{M}$ via the measure change

$$\eta_t = \frac{\mathrm{d}\mathbb{P}}{\mathrm{d}\mathbb{M}}\Big|_{\mathcal{F}_t} = \int_{\mathbb{R}} \frac{f_{U-t}(z - X_t)}{f_U(z)}\, \nu(\mathrm{d}z),\ t < U, \tag{5.8}$$

where $f_t(x)$ is the density function of the underlying Lévy process for all $t \in (0, U]$ and ν is the $\mathbb{P}$-marginal law of the LRB at the terminal date U, the process $\{X_t\}$ is an LRB (the change of measure is singular at U).

Now, returning to the calibrated two-factor log-normal model of section 4.3, but similarly also to the other models in section 4, we may model the drivers $\{X_t^{(1)}\} = \{X_t^{(3)}\}$ and $\{X_t^{(2)}\}$ by two dependent Brownian random bridges under $\mathbb{P}$. The computed $\mathbb{M}$ exposures in figure 9 thus need to be re-weighted by the corresponding amount η_t in order to obtain the $\mathbb{P}$-exposures of the basis swap. Since here we employ LRBs, we have the opportunity to include an expert opinion through the LRB marginals ν as to what level one believes the interest rates will tend to by time U. The re-weighted $\mathbb{P}$-exposures of the basis swap are plotted in the graphs of the right-hand side of figure 9. The maximum of the upper quantile curves shown in the graphs is known as the potential future exposure (PFE) at the level 97.5%.†

Hence, we now have the means to propose a risk-neutral model that can be calibrated to option data and which after an explicit measure change can be applied for risk management purposes while offering a way to incorporate economic views in the dynamic of asset prices. Recalling (2.19) and (5.8), the $\mathbb{Q}$-to-$\mathbb{P}$ measure change is obtained by

$$\frac{\mathrm{d}\mathbb{P}}{\mathrm{d}\mathbb{Q}}\Big|_{\mathcal{F}_t} = \frac{\eta_t}{\mu_t}, \tag{5.9}$$

and the pricing formula for financial assets (2.1) may be utilized under the various measures as follows:

$$\begin{aligned} S_{tT} &= \frac{1}{D_t}\mathbb{E}^{\mathbb{Q}}[D_T\, S_{TT} \mid \mathcal{F}_t] = \frac{1}{D_t\,\mu_t}\mathbb{E}^{\mathbb{M}}[D_T\,\mu_T\, S_{TT} \mid \mathcal{F}_t] \\ &= \frac{1}{h_t}\mathbb{E}^{\mathbb{M}}[h_T\, S_{TT} \mid \mathcal{F}_t] \\ &= \frac{\eta_t}{D_t\,\mu_t}\mathbb{E}^{\mathbb{P}}\left[\frac{D_T\,\mu_T}{\eta_T}\, S_{TT}\,\middle|\,\mathcal{F}_t\right] = \frac{1}{\pi_t}\mathbb{E}^{\mathbb{P}}[\pi_T\, S_{TT} \mid \mathcal{F}_t], \end{aligned} \tag{5.10}$$

for $0 \le t \le T < U$ (since we consider price models driven by LRBs). It follows that the pricing kernel is given by $\pi_t = D_t\,\mu_t\,\eta_t^{-1} = \eta_t^{-1}\,h_t$. Measure changes from a risk-neutral to the real-world probability measure are discussed for similar applications also elsewhere. For a recent study in this area of research, we refer to, e.g. Hull *et al.* (2014).

5.2.2. BSDE-based computations. The BSDE (5.5)–(5.6) can be solved numerically by simulation/regression schemes similar to those used for the pricing of American-style options, see Crépey *et al.* (2013), and Crépey *et al.* (2015). Since in (5.7) we have $\lambda_t = \tilde{\lambda}_t$, the coefficients of the terms $(P_t - \tilde{\vartheta}/(h_t k_t) - \Gamma_t)^{\pm}$ coincide in (5.6). This is the case of a 'linear TVA' where the coefficient $\tilde{f}_t$ depends linearly on $\tilde{\vartheta}$. The results emerging from the numerical BSDE scheme for (5.6) can thus be verified by a standard Monte Carlo computation. Table 1 displays the value of the TVA and its CVA, DVA and LVA components at time zero, where the components are obtained by substituting for ϑ, in the respective term of (5.6), the TVA process $\tilde{\Theta}_t$ computed by simulation/regression in the first place (see section 5.2 in Crépey *et al.* (2013) for the details of this procedure). The sum of the CVA, DVA and LVA, which in theory equals the TVA, is shown in the sixth column. Therefore, columns two, six and seven yield three different estimates for $\tilde{\Theta}_0 = \Theta_0$. Table 2 displays the relative differences between these estimates, as well as the Monte Carlo confidence interval in a comparable scale, which is shown in the last column. The TVA repriced by the sum of its components is more accurate than the regressed TVA. This observation is consistent with the better performance of Longstaff and Schwartz (2001) when compared with Tsitsiklis and Van Roy (2001) in the case of American-style option pricing by Monte Carlo methods, see Chapter 10 in Crépey (2013), for example.

In table 3, in order to compare alternative CSA specifications, we repeat the above numerical implementation in each of the following four cases, with $\bar{\lambda}_t$ set equal to the constant 4.5% everywhere and all other parameters as in (5.7):

$$\begin{aligned} &(1)\ (\bar{R}_b, R_b, R_c) = (100, 40, 40)\%, \quad Q = P,\ \Gamma = 0, \\ &(2)\ (\bar{R}_b, R_b, R_c) = (100, 40, 40)\%, \quad Q = P,\ \Gamma = Q = P, \\ &(3)\ (\bar{R}_b, R_b, R_c) = (40, 40, 40)\%, \quad Q = P,\ \Gamma = 0, \\ &(4)\ (\bar{R}_b, R_b, R_c) = (100, 100, 40)\%, \quad Q = P,\ \Gamma = 0. \end{aligned} \tag{5.11}$$

Remembering that the $t = 0$ value of both legs of the basis swap is equal to EUR 27.96, the numbers in table 3 may seem quite small, but one must also bear in mind that the toy model that is used here doesn't account for any wrong-way risk effect (see Crépey and Song (2015)). In fact, the most informative conclusion of the table is the impact of the choice of the parameters on the relative weight of the different XVA components.

5.2.3. Exposure-based computations. In addition to their use for the computation of PFE, the exposures in section 5.2 can be applied to compute CVA, DVA and LVA. Let us restrict attention to the case of interest rate derivatives with $\{P_t\}$ adapted with respect to $\{\mathcal{F}_t^{(1,2,3)}\}$. We introduce $c(s) = \prod_{i\ge 4} c_i(s)$ and the function of time

$$\begin{aligned} EPE(s) &:= \mathbb{E}^{\mathbb{M}}\left[h_s P_s^+\right] = \mathbb{E}^{\mathbb{Q}}\left[D_s P_s^+\right], \text{ resp. } \mathbb{E}^{\mathbb{M}}\left[h_s P_s^-\right] \\ &= \mathbb{E}^{\mathbb{Q}}\left[D_s P_s^-\right], \end{aligned}$$

called the expected positive exposure, resp. expected negative exposure. For an interest rate swap, the EPE and ENE correspond to the mark-to-market of swaptions with maturity

†In fact, people rather consider the expected positive exposure (expectation of the positive part of the price rather than the price) in the PFE computation, but the methodology is the same.

Table 1. TVA at time zero and its decomposition (all quoted in EUR) computed by regression for $m = 10^4$ or 10^5 against $X_t^{(1)}$ and $X_t^{(2)}$. *Column 2*: TVA Θ_0. *Columns 3 to 5*: CVA, DVA, LVA at time zero repriced individually by plugging $\tilde{\Theta}_t$ for $\tilde{\vartheta}$ in the respective term of (5.6). *Column 6*: Sum of the three components. *Column 7*: TVA computed by a standard Monte Carlo scheme.

m	Regr TVA	CVA	DVA	LVA	Sum	MC TVA
10^4	0.0447	0.0614	−0.0243	0.0067	0.0438	0.0438
10^5	0.0443	0.0602	−0.0234	0.0067	0.0435	0.0435

Table 2. Relative errors of the TVA at time zero corresponding to the results of table 1. 'A/B' represents the relative difference $(A - B)/B$. 'CI//|MC|', in the last column, refers to the half size of the 95% Monte Carlo confidence interval divided by the absolute value of the standard Monte Carlo estimate of the TVA at time zero.

m	Sum/TVA (%)	TVA/MC (%)	Sum/MC (%)	CI//|MC| (%)
10^4	−2.0114	2.0637	0.0108	9.7471
10^5	−1.7344	1.7386	−0.0259	2.9380

Table 3. TVA at time zero and its decomposition (all quoted in EUR) computed by regression for $m = 10^5$ against $X_t^{(1)}$ and $X_t^{(2)}$. *Column 2*: TVA Θ_0. *Columns 3 to 5*: CVA, DVA and LVA at time zero, repriced individually by plugging $\tilde{\Theta}_t$ for $\tilde{\vartheta}$ in the respective term of (5.5). *Column 6*: Sum of the three components. *Column 7*: Relative difference between the second and the sixth columns.

Case	Regr TVA	CVA	DVA	LVA	Sum	Sum/TVA (%)
1	0.0776	0.0602	−0.0234	0.0408	0.0776	−0.0464
2	0.0095	0.0000	0.0000	0.0092	0.0092	−3.6499
3	0.0443	0.0602	−0.0234	0.0067	0.0435	−1.7344
4	0.0964	0.0602	0.0000	0.0376	0.0978	1.4472

s written on the swap, which can be recovered analytically if available in a suitable model specification. In general, the EPE/ENE can be retrieved numerically by simulating the exposure.

In view of (5.5)–(5.6), by the time $t = 0$ forms of (2.34) and (2.35), the non-collateralized CVA at $t = 0$ satisfies (for $R_c \neq 1$, otherwise $CVA_0 = 0$):

$$\begin{aligned}\frac{1}{(1-R_c)}CVA_0 &= \mathbb{E}^{\mathbb{M}}\left[\int_0^T h_s k_s \gamma_s^c P_s^+ \mathrm{d}s\right]\\ &= \int_0^T \mathbb{E}^{\mathbb{M}}\left[h_s P_s^+\right]\mathbb{E}^{\mathbb{M}}\left[k_s \gamma_s^c\right]\mathrm{d}s\\ &= \int_0^T \mathbb{E}^{\mathbb{M}}\left[h_s P_s^+\right]\mathbb{E}^{\mathbb{Q}}\left[Z_s \gamma_s^c\right]\mathrm{d}s\\ &= -\int_0^T EPE(s)\left(\frac{\dot{c}_6(s)}{c_6(s)} + \frac{\dot{c}_4(s)}{c_4(s)}\right)c(s)\mathrm{d}s.\end{aligned}$$

Similarly, for the DVA (for $R_b \neq 1$, otherwise $DVA_0 = 0$) we have:

$$\frac{1}{(1-R_b)}DVA_0 = -\int_0^T ENE(s)\left(\frac{\dot{c}_6(s)}{c_6(s)} + \frac{\dot{c}_4(s)}{c_4(s)}\right)c(s)\mathrm{d}s.$$

For the basis swap of section 5.2 and the counterparty-risk data (5.7), we obtain by this manner $CVA_0 = 0.0600$ and $DVA_0 = -0.0234$, quite consistent with the corresponding entries of the second row (i.e. for $m = 10^5$) in table 1. As for the LVA, to simplify its computation, one may be tempted to neglect the non-linearity that is inherent to $lva_t(\vartheta)$ (unless $\tilde{\lambda}_t = \lambda_t$), replacing ϑ by 0 in $lva_t(\vartheta)$. Then, assuming $lva_t(0) \in \mathcal{X}_t^{(1,2,3)}$, by (5.1)–(5.2), one can compute a linearized LVA at time zero given by

$$\begin{aligned}\widehat{LVA}_0 &= \mathbb{E}^{\mathbb{M}}\left[\int_0^T h_s k_s\, lva_s(0)\mathrm{d}s\right]\\ &= \int_0^T \mathbb{E}^{\mathbb{M}}\left[h_s\, lva_s(0)\right]\mathbb{E}^{\mathbb{M}}\left[k_s\right]\mathrm{d}s\\ &= \int_0^T \mathbb{E}^{\mathbb{M}}\left[h_s\, lva_s(0)\right]c(s)\mathrm{d}s,\end{aligned}$$

by (2.34) for $t = 0$. This is based on the expected (linearized) liquidity exposure

$$\mathbb{E}^{\mathbb{M}}\left[h_s lva_s(0)\right] = \mathbb{E}^{\mathbb{Q}}\left[D_s lva_s(0)\right].$$

In case of no collateralization ($\Gamma_t = 0$) and of deterministic $\tilde{\lambda}_t$ and λ_t, we have

$$\begin{aligned}lva_s(0) &= \tilde{\lambda}_s P_s^+ - \lambda_s P_s^-,\ \widehat{LVA}_0\\ &= \int_0^T \left(\tilde{\lambda}_s EPE(s) - \lambda_s ENE(s)\right)c(s)\mathrm{d}s.\end{aligned}$$

In case of continuous collateralization ($\Gamma_t = P_t$) and of deterministic $\bar{b}_t$ and b_t, the formulas read

$$\begin{aligned}lva_s(0) &= \bar{b}_s P_s^+ - b_s P_s^-,\ \widehat{LVA}_0\\ &= \int_0^T \left(\bar{b}_s EPE(s) - b_s ENE(s)\right)c(s)\mathrm{d}s.\end{aligned}$$

As for CVA/DVA, the LVA exposure is controlled by the

EPE/ENE functions, but for different 'weighting functions', depending on the CSA. For instance, for the data (5.7), the LVA on the basis swap of section 5.2 (collateralized or not, since in this case $\bar{b}_t = b_t = \tilde{\lambda}_t = \lambda_t = 1.5\%$), we obtain $\widehat{LVA}_0 = 0.0098$, quite different in relative terms (but these are small numbers) from the exact (as opposed to linearized) value of 0.0067 in table 1.

6. Conclusion

So far, most of the work on (linear-)rational interest rate and pricing (kernel) models has focused on the relevance of these models from the viewpoint of economics. The transparent relation between model specifications under the risk-neutral and the real-world probability measures provided by the underlying pricing kernel structure has been appreciated for some time. This paper emphasizes the appeal of these models also from the perspective of financial engineering. Models with rational form provide particularly tractable interest rate models, which can be readily extended to multi-curve interest rate models while retaining tractability. These multi-curve models (i) can be efficiently calibrated to swaption data and are particularly easy to simulate since their market factors are deterministic functions of basic processes such as Brownian motions, (ii) require no jumps to be introduced in their dynamics in order to achieve acceptable calibration accuracy, where we recall that traders dislike models with jumps from a hedging perspective. In addition, (iii) the same class of rational models allows for the development of manageable credit-intensity models necessary for the analysis of counterparty-risk valuation adjustments and (iv) the transparent relation between the measures $\mathbb{P}$ and $\mathbb{Q}$ is employed to derive counterparty-risk pricing adjustments (under $\mathbb{Q}$) that are consistent with sound risk-measure computations (under $\mathbb{P}$).

Acknowledgements

The authors thank L. Capriotti, M. A. Crisafi, C. Cuchiero, C. A. Garcia Trillos and Y. Jiang for useful discussions and participants of the first Financial Mathematics Team Challenge, University of Cape Town (July 2014), the fifth International Conference of Mathematics in Finance, Kruger Park, South Africa (August 2014) and of the London-Paris Bachelier Workshop, Paris, France (September 2014) for their helpful comments. The authors also thank two anonymous referees for their proposed improvements. The research of S. Crépey benefited from the support of the 'Chair Markets in Transition' under the aegis of Louis Bachelier Laboratory, a joint initiative of École Polytechnique, Université d'Évry Val d'Essonne and Fédération Bancaire Française.

Disclosure statement

No potential conflict of interest was reported by the authors.

References

Akahori, J., Hishida, Y., Teichmann, J. and Tsuchiya, T., A heat kernel approach to interest rate models. *Jpn. J. Ind. Appl. Math.*, 2014, **31**(2), 419–439. doi:10.1007/s13160-014-0147-3.

Barndorff-Nielsen, O.E., Normal inverse Gaussian distributions and stochastic volatility modelling. *Scand. J. Stat.*, 1997, **24**, 1–13.

Bianchetti, M., Two curves, one price. *Risk Magazine*, 2010, August, 74–80.

Bianchetti, M. and Moreni, M. (Eds.), *Interest Rate Modelling after the Financial Crisis*, 2013 (Risk Books: London).

Bielecki, T.R., Jeanblanc, M. and Rutkowski, M., *Credit Risk Modeling*, 2009 (Osaka University Press, Osaka University CSFI Lecture Notes Series 2: Osaka).

Brigo, D. and Mercurio, F., *Interest Rate Models—Theory and Practice: With Smile, Inflation and Credit*, 2006 (Springer Verlag: Heidelberg).

Brigo, D., Moreni, M. and Pallavicini, A., *Counterparty Credit Risk, Collateral and Funding: With Pricing Cases For All Asset Classes*, 2013 (Wiley: Chichester).

Brody, D.C. and Hughston, L.P., Chaos and coherence: A new framework for interest-rate modelling. *Proc. R. Soc. A*, 2005, **460**(2041), 85–110.

Brody, D.C., Hughston, L.P. and Mackie, E., General theory of geometric Lévy models for dynamic asset pricing. *Proc. R. Soc. A*, 2012, **468**, 1778–1798.

Cheng, S. and Tehranchi, M.R., Polynomial models for interest rates and stochastic volatility, 2014, arXiv:1404.6190.

Cont, R. and Tankov, P., *Financial Modelling with Jump Processes*, 2003 (Chapman and Hall/CRC Press: London).

Crépey, S., Bilateral counterparty risk under funding constraints—Part II: CVA. *Math. Finance*, 2012, **25**(1), 23–50.

Crépey, S., *Financial Modeling: A Backward Stochastic Differential Equations Perspective*, 2013 (Springer Finance Textbooks).

Crépey, S., Bielecki, T.R. and Brigo, D., *Counterparty Risk and Funding—A Tale of Two Puzzles*, 2014 (Chapman and Hall/CRC Financial Mathematics Series: Boca Raton, FL).

Crépey, S., Gerboud, R., Grbac, Z. and Ngor, N., Counterparty risk and funding: The four wings of the TVA. *Int. J. Theor. Appl. Finance*, 2013, **16**(2), 1350006.

Crépey, S., Grbac, Z., Ngor, N. and Skovmand, D., A Lévy HJM multiple-curve model with application to CVA computation. *Quant. Finance*, 2015, **15**(3), 401–419.

Crépey, S. and Song, S., *Counterparty Risk and Funding: Immersion and Beyond*, LaMME preprint, 2015 (available on HAL).

Cuchiero, C., Fontana, C. and Gnoatto, A., A general HJM Framework for multiple yield curve modeling, 2014, arXiv:1406.4301v1.

Cuchiero, C., Keller-Ressel, M. and Teichmann, J., Polynomial processes and their applications to mathematical finance. *Finance Stoch.*, 2012, **16**(4), 711–740.

Döberlein, F. and Schweizer, M., On savings accounts in semimartingale term structure models. *Stoch. Anal. Appl.*, 2001, **19**, 605–626.

Eberlein, E., Glau, K. and Papapantoleon, A., Analysis of Fourier transform valuation formulas and applications. *Appl. Math. Finance*, 2010, **17**, 211–240.

El Karoui, N., Peng, S. and Quenez, M.-C., Backward stochastic differential equations in finance. *Math. Finance*, 1997, **7**, 1–71.

Filipović, D., Larsson, M. and Trolle, A.B., Linear-rational term stucture models, 2014. SSRN:2397898.

Filipović, D. and Trolle, A.B., The term structure of interbank risk. *J. Financ. Econ.*, 2013, **109**, 707–733.

Flesaker, B. and Hughston, L.P., Positive interest. *Risk Magazine*, 1996, **9**, 46–49.

Fujii, M., Shimada, Y. and Takahashi, A., A note on construction of multiple swap curves with and without collateral. *FSA Res. Rev.*, 2010, **6**, 139–157.

Fujii, M., Shimada, Y. and Takahashi, A., A market model of interest rates with dynamic basis spreads in the presence of collateral and multiple currencies. *Wilmott Magazine*, 2011, **54**, 61–73.

Heath, D., Jarrow, R. and Morton, A., Bond pricing and the term structure of interest rates: A new methodology for contingent claims valuation. *Econometrica*, 1992, **60**, 77–105.

Henrard, M., The irony in the derivatives discounting. *Wilmott Magazine*, 2007, **30**, 92–98.

Henrard, M., The irony in the derivatives discounting part II: The crisis. *Wilmott Magazine*, 2010, **2**, 301–316.

Henrard, M., *Interest Rate Modelling in the Multi-curve Framework*, 2014 (Palgrave Macmillan: Basingstoke).

Hoyle, E., Hughston, L.P. and Macrina, A., Lévy random bridges and the modelling of financial information. *Stoch. Process. Appl.*, 2011, **121**, 856–884.

Hughston, L.P. and Rafailidis, A., A chaotic approach to interest rate modelling. *Finance Stoch.*, 2005, **9**, 43–65.

Hull, J.C., Sokol, A. and White, A., Modelling the short rate: The real and risk-neutral worlds, 2014. Available online at: http://dx.doi.org/10.2139/ssrn.2403067.

Hunt, P. and Kennedy, J., *Financial Derivatives in Theory and Practice*, revised ed., 2004 (Wiley: New York).

Kenyon, C., Short-rate pricing after the liquidity and credit shocks: Including the basis. *Risk Magazine*, 2010, November, 83–87.

Kijima, M., Tanaka, K. and Wong, T., A multi-quality model of interest rates. *Quant. Finance*, 2009, **9**(2), 133–145.

Longstaff, F.A. and Schwartz, E.S., Valuing American options by simulations: A simple least-squares approach. *Rev. Financ. Stud.*, 2001, **14**(1), 113–147.

Macrina, A., Heat kernel models for asset pricing. *Int. J. Theor. Appl. Finance*, 2014, **17**(7), 1–34.

Macrina, A. and Parbhoo, P.A., Randomised mixture models for pricing kernels. *Asia-Pac. Financ. Markets*, 2014, **21**, 281–315.

Mercurio, F., A LIBOR market model with stochastic basis. *Risk Magazine*, 2010a, December, 84–89.

Mercurio, F., Interest rates and the credit crunch: New formulas and market models. Technical report, Bloomberg Portfolio Research Paper No. 2010-01-FRONTIERS, 2010b.

Mercurio, F., Modern LIBOR market models: Using different curves for projecting rates and for discounting. *Int. J. Theor. Appl. Finance*, 2010c, **13**, 113–137.

Moreni, N. and Pallavicini, A., Parsimonious multi-curve HJM modelling with stochastic volatility. In *Interest Rate Modelling After the Financial Crisis*, edited by M. Bianchetti and M. Moreni, pp. 393–416, 2013 (Risk Books: London).

Moreni, N. and Pallavicini, A., Parsimonious HJM modelling for multiple yield-curve dynamics. *Quant. Finance*, 2014, **14**(2), 199–210.

Nguyen, T. and Seifried, F., The multi-curve potential model, 2014. Available online at: http://ssrn.com/abstract=2502374.

Parbhoo, P.A., Information-driven pricing kernel models. PhD Thesis, University of the Witwatersrand, 2013.

Rogers, L.C.G., The potential approach to the term structure of interest rates and foreign exchange rates. *Math. Finance*, 1997, **7**, 157–176.

Rutkowski, M., A note on the Flesaker–Hughston model of the term structure of interest rates. *Appl. Math. Finance*, 1997, **4**, 151–163.

Tsitsiklis, J.N. and Van Roy, B., Regression methods for pricing complex American-style options. *IEEE Trans. Neural Networks*, 2001, **12**, 694–703.